Pulsed Active Steering Hardware-in-the-Loop Experiment

by

Akram Abdel-Rahman

A thesis
presented to the University of Waterloo
in fulfillment of the
thesis requirement for the degree of
Master of Applied Science
in
Mechanical Engineering

Waterloo, Ontario, Canada, 2009

I hereby declare that I am the sole author of this thesis. This is a true copy of the thesis, including any required final revisions, as accepted by my examiners.

I understand that my thesis may be made electronically available to the public.

Abstract

Active safety vehicle systems are continuously being researched to make vehicles safer to drive. Active steering is a new active safety system that involves controlling the vehicle steering angle during the vehicle's loss of stability. The steering signal, which an active steering system intervenes with, is brought to study in this thesis. Using a pulsed signal instead of a constant signal as the output of an active steering system arises new areas to study. This thesis focuses on the effect that the different pulse parameters have on the yaw and roll dynamics of a passenger vehicle. The parameters of a pulse consist of its frequency, amplitude, and pattern.

Simulations were done with different vehicle models in different simulation softwares to assess the effect that each of the pulse parameters has on the vehicle dynamics. These simulation softwares include DynaFlexPro, Matlab/Simulink and Adams/Car. In addition, a whole test bed was designed and assembled to carry out Hardware-In-the-Loop (HIL) simulation experiments involving active steering systems. The test bed was used to firstly validate the results obtained from the simulations, and secondly to assess the applicability of a pulsed active steering system. Conclusions of the obtained results as well as future work are mentioned at the end of this thesis.

Acknowledgements

I would like to thank my supervisors, Amir Khajepour and John McPhee. Their guidance for this research project as well as their good character made working under their supervision convenient. I would also like to thank Roel Vos, Tom Uchida and Christoph Baum for the contributions they made towards this project. As a whole I would like to acknowledge the Motion of Research Group (MoRG) for the many assistance they provided throughout the time of this project.

Special thanks also go to the experienced technical staff of the Mechanical Engineering department that helped in putting together the test bed of this research project.

Contents

List of Tables

List of Figures

Chapter 1

Introduction

Some consider vehicles to be weapons of mass destruction if not operated and used correctly. To drive a chunk of mass of around one tonne in weight requires a lot of safety measures to make it affable to fit in any city. Car accidents are statistically in the top ten causes of death in the U.S.A as stated by CDC (Centers for Disease Control and Prevention) [2]. That is why governments, as well as other institutions are placing higher demands for vehicle safety on the automotive industry. Active safety control systems are regularly being researched to optimize their efficiency to prevent all kinds of accidents to occur. Not all car accidents initiate from the same problem, but the loss of car handling and stability is certainly considered to be a main cause of car accidents.

Different active safety control systems have different roles. As well, some of them are still in the introductory phase in the automotive market or are still being researched whereas others are considered to be a mandatory requirement for any new car model.

Starting this year, 2009, the National Highway Traffic Safety Authority (NHTSA) is carrying out a plan to make Electronic Stability Control (ESC) a mandatory requirement by the year 2012 on all passenger vehicles in the United States. ESC is an active safety system that improves vehicle stability by monitoring and preventing skids as well as other forms of instability. It does so by controlling independent brake forces on each tire as well as (not always) the engine throttle. ESC systems are named differently amongst automotive companies. Electronic Stability Program (ESP) (such as in Audi, Mercedes, Volkswagen models), Dynamic Stability Control (DSC) (such as in BMW, Mazda models) are examples of ESC systems given a trademark name.

An intensive study has shown that by making ESC systems mandatory on all passenger vehicles car accidents will be reduced significantly. The study shows a potential of decreasing all single-vehicle crashes by a significant amount of 34%, as well as reducing all rollover crashes by 71%.

Although ESC systems show that they will have a positive impact on reducing car accidents, research has shown that the active safety system will be weak, or have

a low effect if any, in preventing car accidents in certain driving circumstances. By having the brakes and engine throttle monitored by ESC, the only other input variable that is not yet monitored is the driver's steering input. There are many circumstances that the driver wrongly controls the steering of the vehicle such as how to deal with oversteering during a driving maneuver (which requires a great deal of driving experience) or when to limit the steering wheel angle to prevent rollover from taking place. Such reasoning introduced a new active safety system: Active steering.

Active steering adjusts the steering angle of the vehicle by adding a controlled steering angle to the driver's steering input. The active system will only operate during extreme conditions to prevent instability of the vehicle. Active steering systems are currently installed in some passenger car, such as BMW's 5-series, although they are used for other purposes alongside vehicle stability (such as variable steering ratio) [16]. In the context of vehicle dynamic stability, active steering deals explicitly with preventing the fatal incident of a rollover as well as reducing the deviation of a vehicle from its desired path.

This research is to assess the effect as well as the applicability of having a pulse active steering controller signal. The idea is analogous to that of an ABS (Anti-lock Braking System). Once ABS is engaged the braking force becomes pulsed which research has shown to have more benefits when compared to conventional braking systems.

This research was divided into two major parts. The first part was to assess the effect of the new pulse phenomena through state-of-the-art simulation softwares. Various vehicle models as well as different simulation softwares were used in this approach. The effects pulse active steering had on the yaw as well as the roll dynamics of the vehicle were observed. Furthermore, the sole effect of each of the pulse's parameters; amplitude, frequency, and pulse pattern had on the vehicle dynamics were assessed.

The second part was to assess the applicability of the active safety system by building a test bed for a Hardware-in-the-Loop simulation experiment. The test bed consists of a steering system that allows two steering inputs to be added or subtracted from each other as shown in Figure 1.1. The test bed was designed such that it accommodates future work relating to active steering. This was an important part of this project and therefore some design aspects of the various subsystems will be presented. Values obtained from simulations were used to help size components used in the test bed. The test bed was designed such that a user could drive the virtual vehicle model and a pulsed active steering controller would intervene during instable situations. The experiment was used to verify the simulation results as well as to show the applicability of pulse active steering.

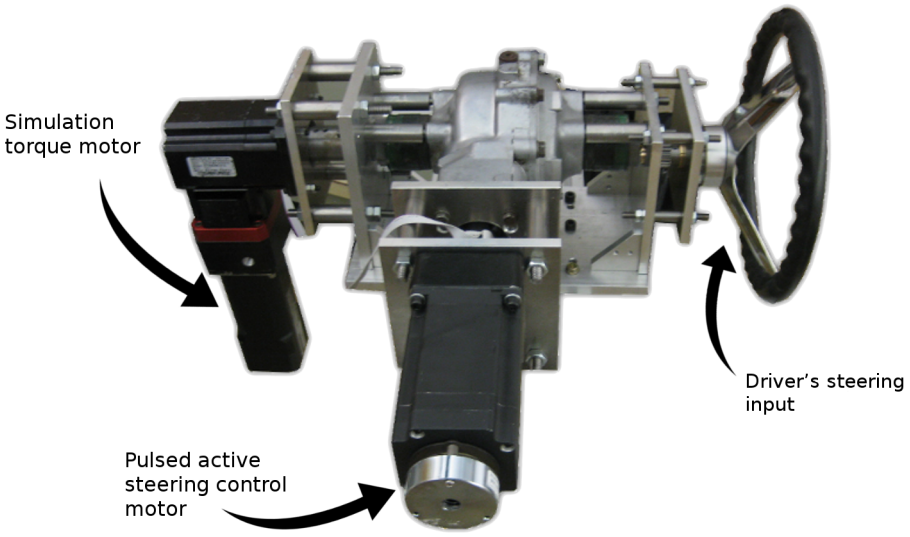

Figure 1.1: HIL simulation experiment setup

Chapter 2

Background

This chapter presents the background knowledge to this research project. The literature review as well as an introduction to the different simulation software used will be presented in separate sections.

2.1 Literature Review

2.1.1 Vehicle Stability Active Systems

The purpose of a vehicle stability active system is primarily, but not limited, to produce a compensating torque for yaw and roll disturbances. The method in which this is achieved could vary but at the end the active system should be dependable and efficient. As stated in [20], the main objectives of any stability active system in vehicles is to respond in the range of the driver's reaction time to prevent loss of vehicle control as well as follow the driver's desired path of travel.

One of the first active stability control system that made it to the automotive market and is found in all passenger cars today is the Antilock Braking System (ABS). ABS prevents the wheels of the vehicle to lock by giving pulsed break signals to all four wheels. This will allow the driver to keep steering control under heavy breaking and in some cases shorten breaking distances. Although ABS has gained worldwide acceptance and is today considered to be a mandatory option in vehicles, its effect covers a small portion of all vehicle instability cases.

The Electronic Stability Control system (ESC) as well was an early stability active system to be introduced. This stability control system was feasible and did not require any major hardware alterations than that already existing in the vehicle because it uses the components of the ABS. ESC operates by giving out independent braking signals to each wheel as well as controlling the engine throttle so that a compensating torque is produced for yaw disturbances. It also showed positive results in lowering the possibility of the vehicle to rollover in extreme driving maneuvers. The work of S.Horiuchi [14] shows the great results of using this

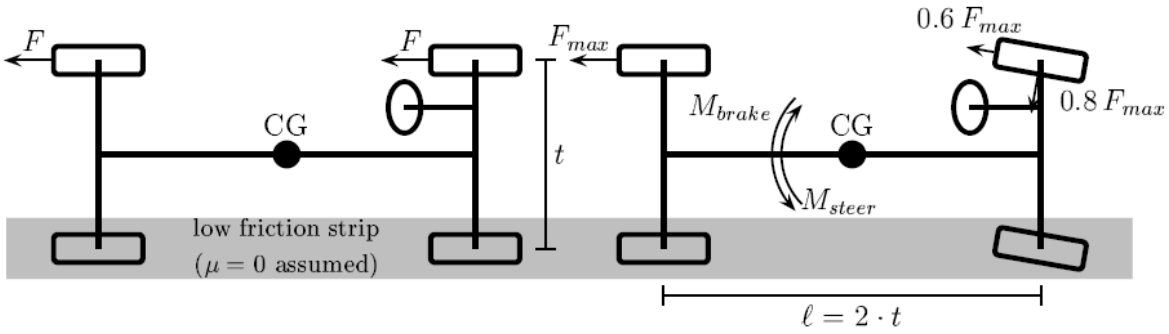

Figure 2.1: A μ-split road with and without active steering (left is without active steering control)

active system but also highlights its limitations in certain conditions. Research is being done to improve ESC regularly to overcome these limitations. The dependence of the active system improved with research but has not yet reached complete dependence for all kinds of driving situations.

By having ESC using the engine throttle and the braking system for stability, the only other system that is available and not yet used for active stability is the steering system. The active safety system for steering is commonly known as active steering. Active steering was first introduced in the late 1960's. Kasselmann and Keranen [15] designed an active control system that measures the yaw rate by a gyroscope and uses proportional feedback to generate an additional steering input for all four wheels. Although this first study was done on a four-wheel steering vehicle, other studies emerged focusing on rear-wheel and front wheel steering vehicles. These studies found that active steering will have a positive effect on both yaw and roll stability.

Many authors started comparing between active rear steering (ARS), active front steering (AFS) and four-wheel steering systems (4WS). In addition, other authors, such as A.Masato [3], started comparing between active steering and ESC and studying the effect of combining both active systems together. Although the ESC does show great results in gaining the vehicle both yaw and roll stability, the addition of active steering control will only improve the efficiency of the active safety systems.

There are driving conditions where the ESC will not be efficient. Ackermann [5] shows the advantages of using active steering control and what it has to offer that ESC cannot. He presented possible cases where ESC will not prevent the vehicle from losing control whereas active steering will. Consider a μ-split road as shown in Figure 2.1. A μ-split situation is when the friction coefficients on the left tires are significantly different from that on the right tires.

Consider the right side of the vehicle to have no friction with the road. By using only ESC, it will not prevent the vehicle from sliding counter clockwise. But with

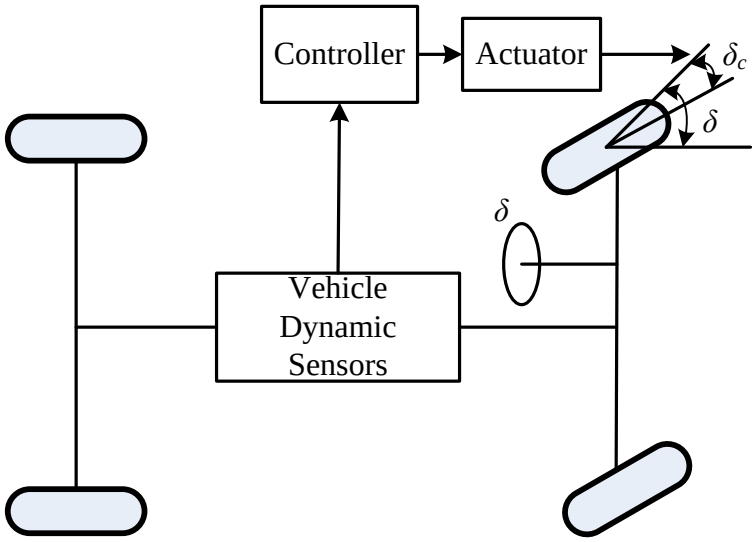

Figure 2.2: Overview of active steering concept

both ESC and active steering the vehicle is kept more stable and the possibility of sliding is lowered.

To summarize, Ackermann stated that combining both active steering and ESC will surpass the limitations that appear if one of the two mentioned active systems is used alone. Similarly, Nagai [23] proposed a study to see the effect of combining active steering and ESC compared to using ESC alone. He concluded that the vehicle dynamics can be much improved by the integrated control system (ESC and active steering) compared with the ESC only. The integrated control system also showed greater robustness to make the actual vehicle response to follow the desired path of travel.

In 1996, E. Ono et al. [24] showed that a simple active front wheel steering (AFS) controller via robust control strategy was capable of improving the yaw rate in a vehicle spin situation. Furthermore, Y. Hirano [13] proposed active rear steering (ARS) via robust control strategy as another method for improving vehicle handling. A year later, W. Sienel [27] proposed another AFS method via estimation of cornering stiffness. Since the late 1990s, many other similar research activities in either active front [20] [12], or rear steering [19] have been presented.

2.1.2 Active Steering Control

To start with, a brief explanation of the active system's operation will be presented. When the vehicle starts to sense the likeliness of loss of stability, a controlled steering angle input is added to the driver's steering input so that the tires are aligned in a way that it would prevent extreme loss of yaw or roll stability.

Figure 2.2 shows a simple control system for an active front steering system.

Vehicle Yaw Dynamics		**Vehicle Roll Dynamics**
States affecting yaw dynamics only	*States affecting yaw and roll dynamics*	*States affecting roll dynamics only*
Yaw rate	Lateral acceleration	Roll rate
	Longitudinal acceleration	Vertical acceleration

Table 2.1: Degrees of freedom affecting the yaw and roll dynamics of the vehicle

Vehicle dynamic sensors embedded in the vehicle constantly monitor the vehicle dynamics to sense for any yaw or roll disturbances. Once any disturbance is observed by the sensors, a signal is fed into the main controller, which is the Engine Control Unit (ECU), that controls the actuator to intervene in the steering input to the vehicle to produce the required dynamic response.

The dynamics of the vehicle that need to be monitored depends on whether roll dynamics or yaw dynamics are of concern. Some vehicle's states affect both the yaw and roll dynamics such as the lateral acceleration of the vehicle. Table 2.1 shows the vehicle's states that affect the yaw and roll dynamics.

All these dynamic states correspond to the center of gravity of the sprung mass of the vehicle. Therefore the sensors used should measure or estimate the dynamic variable at the center of mass. As for the actuator, authors explained that active steering does not necessarily have to wait for steer-by-wire to be implemented. Kramer [17] proposed that for an active front steering system, the actuator could be placed along the steering column such that the control system's intervention is a rotational motion of the steering column (position (1) in Figure 2.3). However, Kasselmann [15] proposed that the actuator is to be placed at the steering rack such that the actuator intervenes with a lateral motion (position (2) in Figure 2.3). As for designing the control system, authors usually design the control system for the yaw motion separately from that of the roll motion. Therefore each of them will be explained separately here.

Yaw motion control by active steering

The active system continuously monitors the longitudinal velocity, steering input of the driver, and the vehicle's yaw rate. By using the longitudinal velocity as well as the steering input the controller is able to evaluate the desired path of travel of the driver. The desired path is then compared with the actual path of travel measured by the yaw rate sensors. If there is a difference more that a certain threshold, the controller generates the additional steering angle to be added to compensate for yaw disturbances [18].

As mentioned in Table 2.1, the yaw dynamics of the vehicle depend on the yaw rate as well as the lateral motion of the vehicle. In [4], a steering control

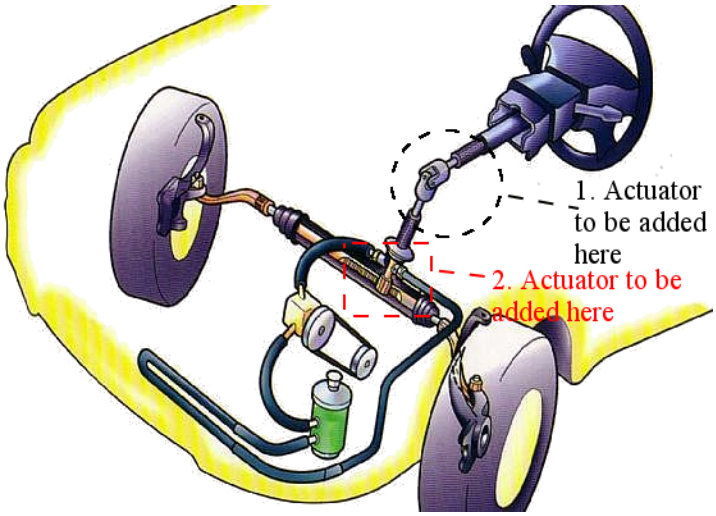

Figure 2.3: Possible locations for active steering actuator

method was presented which achieves robust unilateral decoupling of the vehicle's yaw and lateral motion, i.e. the yaw rate is no longer observable from the lateral acceleration. Remarkable about this method is that the decoupling property holds robustly despite varying operation conditions such as speed, mass of the vehicle, and uncertain road conditions. So far, it provides an advantageous separation of two basic tasks being under the responsibility of the driver: path following and disturbance attenuation. With the robust steering control, the first task is left to the driver but the latter is managed by the active steering system [6]. This makes driving a car easier and provides safety advantages. This method was verified in driving experiments in [7].

Vehicle rollover avoidance by active steering

Driving situations, which can directly induce vehicle rollover, are excessive speed when entering a curve, severe lane change, obstacle avoidance maneuvers or disturbance impacts like side wind gusts. The possibility of a vehicle to rollover greatly depends on the ratio of the track width to the height of the center of gravity, and this is confirmed by accident statistics. A rollover coefficient, R, serves as an indicator of the possibility of a rollover to take place [5]. The stable range of R is between [-1,1]. For R to be equal to 1 or -1 means the vehicle's left or right wheels have, or are about to, lose contact with the ground. R depends on the ratio of the track width and the height of the center of gravity as well as other dynamic states of the center of gravity of the vehicle's sprung mass.

Usually studies on rollover prevention are done by using the integrated control system that consists of active steering and ESC. Tilman et al. [28] use a control system that consists of three feedback loops; emergency active steering, ESC, and normal active steering using a PD controller. This is shown in Figure 2.4.

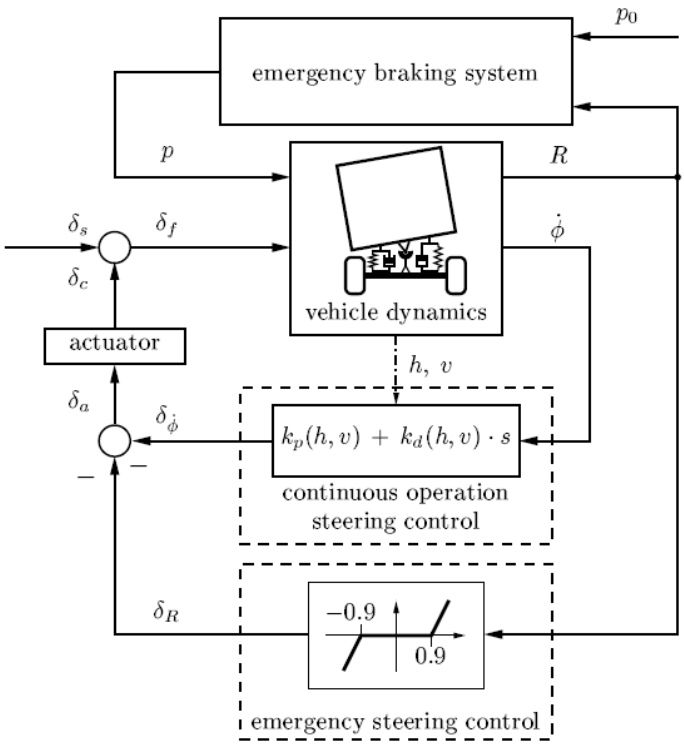

Figure 2.4: Rollover controller structure

In Figure 2.4, δ with its respective subscripts correspond to various steering commands. As well p with its corresponding subscripts correspond to various braking commands. $\dot{\phi}$ and v correspond to the roll rate and the lateral velocity of the vehicle respectively. h is a geometry parameter corresponding to the distance between the roll axis and the sprung mass center of mass. Continuous operation steering control refers to active steering with a PD controller.

When the vehicle is about to rollover this means that the magnitude of R is approaching 1. When this occurs the rollover avoidance is given priority over ideal lane keeping (i.e. following driver's desired path of travel). To emphasize, to drive the sharpest curve which is physically possible, maximum lateral acceleration must be applied and the feasible lateral acceleration is limited by rollover. The relevant boundary is reached if the vehicle is steered such that the inner wheels are just about to lift off the road. The optimal strategy to keep the sharpest curve possible while avoiding rollover would be to keep the vehicle at the rollover limit. As shown in Figure 2.4, the author of [28] chose R=0.9 to be the threshold for this to happen. That means when R reaches or exceeds 0.9, then the difference is fed back through a proportional gain controller to the front wheel steering angle such that the curvature of the course is slightly reduced and rollover is avoided. At the same time deceleration of the vehicle is forced by operation of the brakes to improve

the effect of rollover risk reduction.

A recent study was done by Kuo, [18], where he proposes making the feedback steering input pulsed, the feedback steering input here being δ_R in Figure 2.4 or δ_c in Figure 2.2. Kuo tried comparing different pulse patterns on the performance of the active safety system. Pulsed active steering is assumed to show positive potential because it is analogous to the Antilock Braking System concept. This thesis and research project was intended to assess pulsed active steering further through simulations and Hardware-in-the-loop experiments.

By looking into pulsed active steering, new factors are introduced that require assessment. With respect to Figure 2.5, a pulse could be controlled in different ways, it could be controlled through its frequency ($1/t_T$), amplitude (A), and/or pulse shape (symmetric or assymetric b/a). This research project is to build over Kuo's work. This research project will assess the vehicle dynamics through the control of each of pulse's parameters.

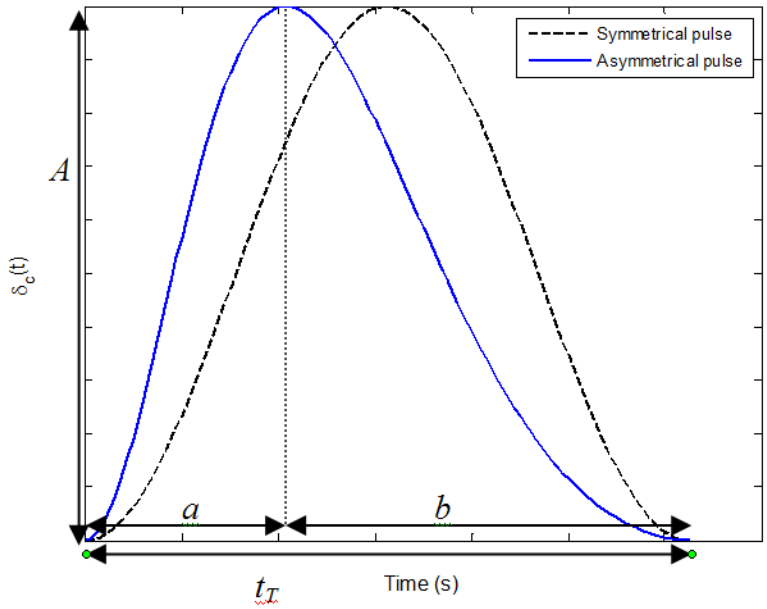

Figure 2.5: Pulse parameters for control

2.2 Simulation Softwares

Vehicle simulation softwares are based on modeling real world vehicle driving situations with a set of mathematical formulas. There are a number of vehicle simulation softwares available, whether they are stand alone applications or toolboxes embedded in software application environments. The softwares used in this research project were Adams/Car, DynaFlexPro (or now MapleSim) and Matlab/Simulink. This section will briefly present each of these simulation software.

2.2.1 Adams/Car

Adams is a family of interactive motion simulation software modules that belong to MSC Software Corporation. Adams core package (Adams/View, Adams/Solver, and Adams/PostProcessor) allow to import geometry from most major CAD systems or to build a solid model of a mechanical system from scratch. A full library of joints and constraints is available for creating articulated mechanisms. Several modules that are part of Adams can be used to accomplish specialized tasks and achieve better fidelity of results. The module used in this research project was Adams/Car which allows you to perform full-vehicle simulation of different driving conditions [1].

2.2.2 DynaFlexPro/MapleSim

DynaFlexPro is a state-of-the-art technology software for modeling mechanical multibody systems which is currently available through MapleSim from Maplesoft. A graphical user interface, DynaFlexPro ModelBuilder, facilitates the rapid creation of system models using block diagrams and drop-down menus. DynaFlexPro combines graph theory with engineering mechanics in algorithms that automatically generate the system equations from the system model. Powerful Maple computer algebra technologies are used to create small and efficient sets of system equations in symbolic form, which allows for viewing, physical insight and sharing [29].

2.2.3 Matlab/Simulink

Matlab, a product of Mathworks, is a high-level language and interactive environment that enables you to perform computationally intensive tasks. Matlab could be used in a wide range of applications, some of which include signal and image processing, communications, control design, and test and measurement. Add-on toolboxes extend the Matlab environment to solve particular classes of problems in these application areas.

Simulink, which is also a product of Mathworks, is an environment for multi domain simulation and Model-Based Design for dynamic and embedded systems. It provides an interactive graphical environment and a customizable set of block libraries that enables you to design, simulate, implement, and test a variety of time-varying systems, including communications, controls, signal processing, video processing, and image processing. Add-on products extend Simulink software to multiple modeling domains, as well as provide tools for design, implementation, and verification and validation tasks.

Simulink is integrated with Matlab, providing immediate access to an extensive range of tools. In this research project, Matlab/Simulink were used to simulate an analytically derived vehicle model through various driving situations. As well, the

Real-Time Workshop toolbox in Simulink was extensively used for the Hardware-in-the-Loop simulation experiments in this research project [30].

Chapter 3

Modeling and Simulation

Accurate vehicle model(s) are essential for obtaining reliable results. Although G. Box was quoted saying, 'All models are false but some are useful' [10], it is important to make sure that the model(s) used fall in the category of the 'useful some' rather than the 'false majority'. This research involved using three separate models each in a different simulation software. This was done due to the different objectives behind each simulation setup. The three models are:

- Analytical hand-derived bicycle model and roll model
- Full vehicle model in Adams/Car vehicle simulation software
- Full vehicle model built in Maple's DynaFlexPro vehicle simulation software

This chapter consists of presenting each model separately. Each simulation set's results will follow the presentation of their respective vehicle model.

3.1 Analytical Model

To hand-derive a vehicle model, there are certain assumptions and approximations that need to be made to simplify the complexity of the equations of motion of a real vehicle. The analytical model consists of a yaw model and a roll model.

3.1.1 Yaw Model

The yaw model used is widely known as the bicycle model. A free body diagram of the model is presented in Figure 3.1. The inertial planar coordinate frame is (X, Y) whereas the body-fixed planar coordinate frame (x, y) is rotated by an angle ψ about the vertical axis (out of the page). $\overline{F_f}, \overline{F_r}$ correspond to the lateral forces of the front and rear tire respectively. $\overline{V}$ is the velocity of the vehicle in the (x, y) plane, whereas

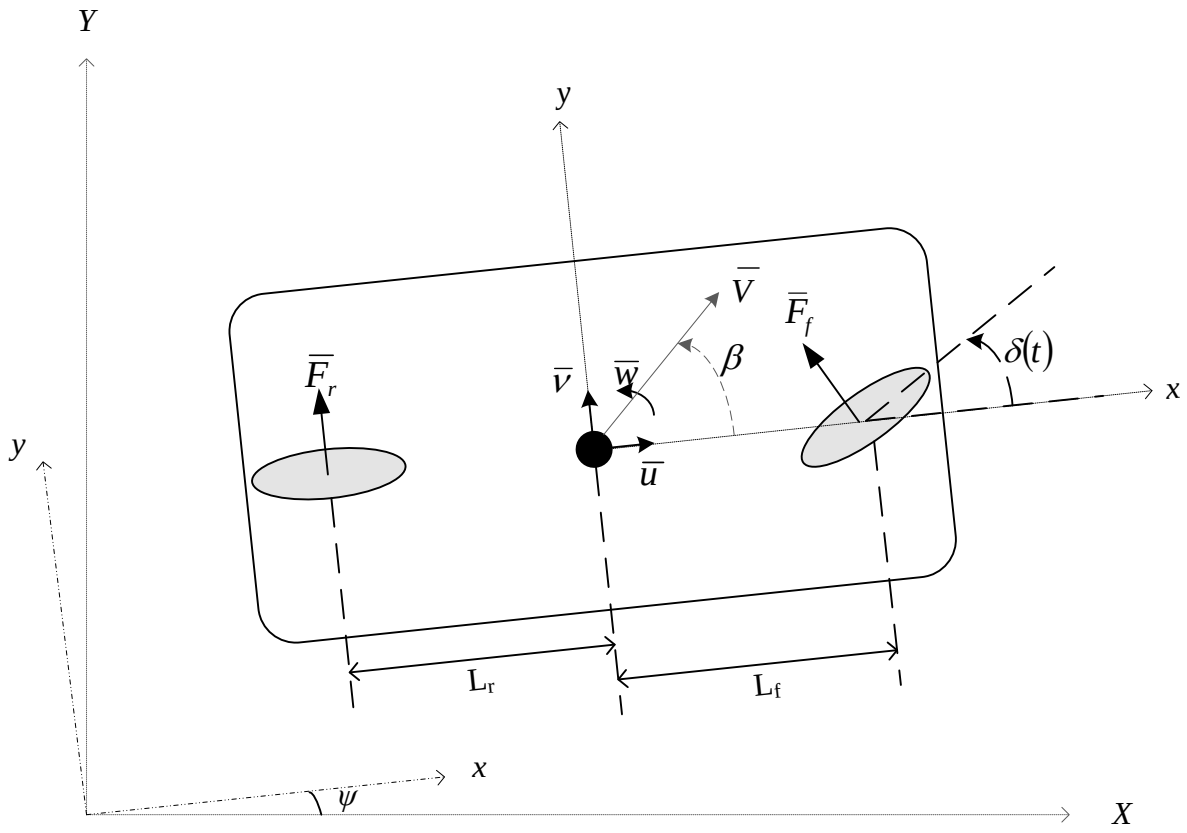

Figure 3.1: Hand-derived yaw model

β represents $\overline{V}$ direction as measured from the positive x axis. The proposed yaw model has three degrees of freedom, they are: the vehicle's longitudinal velocity, lateral velocity and yaw rate denoted in Figure 3.1 as $\overline{u}, \overline{v}$, and $\overline{w}$ respectively. The lengths L_r and L_f represent the distances between the vehicle's center of mass and the rear and front tire respectively.

The following list shows all the assumptions and approximations made to derive yaw model.

1. Model approximated to a linear single track model. (i.e. Planar dynamics model)
2. The two front wheels will be approximated to be a one centered front wheel.
3. The two rear wheels will be approximated to be a one centered rear wheel.
4. A vehicle body fixed reference frame (x, y) will have an origin at the center of mass of the vehicle, with x being the body fixed longitudinal axis.

5. The front and rear centered wheels as well as the center of mass all lie along the vehicle's longitudinal axis. The front wheel will be rotating with respect to the vertical axis, but its center of rotation will be on the x axis for all time.

6. The rear wheel will not have a steering angle (i.e. will always align with the longitudinal axis).

7. The three independent degrees of freedom of the yaw model are the longitudinal velocity $\overline{u}$, the lateral velocity $\overline{v}$, and the yaw rate $\overline{w}$.

8. The longitudinal velocity will be set to be constant (thus lowering the degrees of freedom from three to two). Therefore the longitudinal forces of the tires will be neglected due to having minor effect on the other two degrees of freedom.

9. Wind forces and air drag will be neglected.

The validity of these assumptions could be found in [26], where the author explains thoroughly the effect of these assumptions. The total mass of the yaw model is m, which consists of the sprung and unsprung masses m_1 and m_2 respectively. The mass moment of inertia of the yaw model is I_{zz}. Newton-Euler equations were used to obtain the equations of motion of the model. The subscripts (x, y, z) correspond to the body-fixed coordinate frame. The equation of motion along the y direction was obtained as follows:

$$\sum F_y = m\, a_y \tag{3.1a}$$

$$F_r + F_f \cos\left(\delta\left(t\right)\right) = m\left(\dot{\nu} + 2uw\right) \tag{3.1b}$$

Whereas the equation of motion for rotation about the z axis was obtained as follows:

$$\sum M_z = I_{zz}\alpha_z \tag{3.2a}$$

$$L_f F_f \cos\left(\delta\left(t\right)\right) - L_r F_r = I_{zz}\dot{w} \tag{3.2b}$$

By rearranging equations (3.1b) and (3.2b) in terms of $\dot{\nu}$ and $\dot{w}$ respectively, the following equations of motion are obtained.

$$\dot{\nu} = \frac{1}{m}\left[F_r + F_f \cos\delta(t)\right] - 2uw \tag{3.3a}$$

$$\dot{w} = \frac{1}{I_{zz}}\left[L_f F_f \cos\delta(t) - L_r F_r\right] \tag{3.3b}$$

These equations of motion are observed to be coupled and may appear to be linear in nature. But the linearity of the system greatly depends on the tire model used for the front and rear tires, from which F_f and F_r are obtained. By having linear tire models the equations of motion are said to be linear and linear systems theory could be used. However, this limits the validity of the model and may lead to unrealistic results.

3.1.2 Tire Model

To evaluate the tire forces F_f and F_r in equations (3.3a) and (3.3b) a tire model is required. There are many tire models available in the literature as mentioned earlier, from simple linear models to highly complex sophisticated ones. It is important for this analytical model to compromise between simplicity and the validity of the tire model. For this analytical model the tire model will be used to only calculate the lateral tire forces. A good choice of tire model for this vehicle model will be a model that could represent the lateral tire force in a single equation and yet hold a degree of accuracy.

It was decided that Pacejka's tire model [25] would be a suitable choice for this vehicle model. Pacejka's tire model, commonly known as 'The Magic Formula', has many versions, old to new and simple to complex. The Pacejka tire model used here depends solely on the slip angle to evaluate the tire's lateral force. The front and rear tire slip angles can be obtained through equations (3.4a) and (3.4b) respectively.

$$\theta_f = \delta - \tan^{-1}\left(\frac{\nu + L_f w}{u}\right) \tag{3.4a}$$

$$\theta_r = -\tan^{-1}\left(\frac{\nu - L_r w}{u}\right) \tag{3.4b}$$

The following equations are the nonlinear lateral tire forces with respect to the slip angles.

$$F_f = D_f \sin\left[C_f \tan^{-1}\left(B_f\left(1 - E_f\right)\theta_f + E_f \tan^{-1}\left(B_f\theta_f\right)\right)\right] \tag{3.5a}$$

$$F_r = D_r \sin\left[C_r \tan^{-1}\left(B_r\left(1 - E_r\right)\theta_r + E_r \tan^{-1}\left(B_r\theta_r\right)\right)\right] \tag{3.5b}$$

Where the constants B, C, D, and E represent certain properties and conditions of the tire [25]. Equations (3.5a) and (3.5b) could be further linearized to become Equations (3.6a) and (3.6b). The linearized model would be useful as it enables

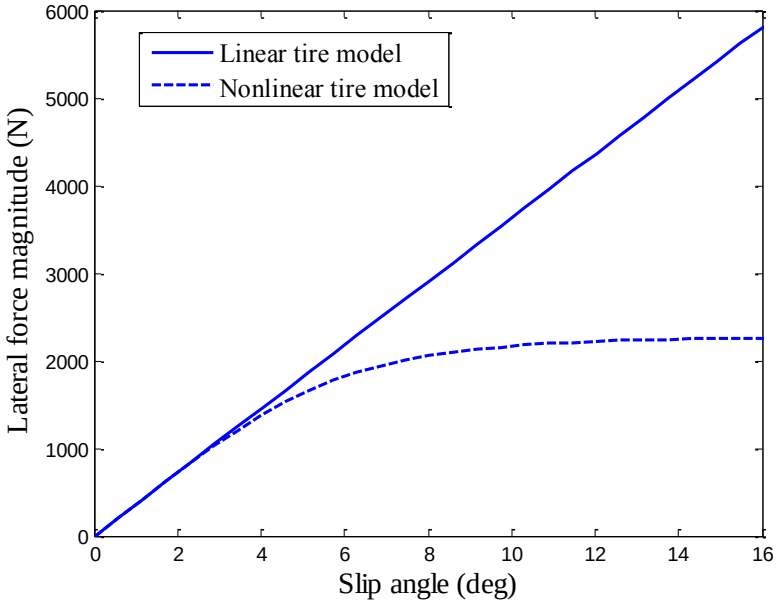

Figure 3.2: Linear and nonlinear lateral force tire models

the use of linear systems theory but at the cost of lower validity and less reliable results.

$$F_f = D_f C_f B_f \theta_f \tag{3.6a}$$
$$F_r = D_r C_r B_r \theta_r \tag{3.6b}$$

Figure 3.2 shows a plot of the linear and nonlinear tire models against the tire's lateral slip angle.

3.1.3 Roll Model

The roll model of the vehicle is used in parallel with the previously presented yaw model to derive the vehicle's roll equations of motion. Figure 3.3 shows a free body diagram of the roll model used, viewed from the front side of the vehicle (in the $-x$ direction).

The roll angle ϕ is the angle of rotation about x between the inertial coordinate Z and the body-fixed coordinate z. m_1 and m_2 are, as defined previously, the sprung and unsprung masses of the vehicle respectively. The center of gravity of the unsprung mass is assumed to be level with the road as shown in Figure 3.3. The distance between the road and the roll axis measured along Z is defined by h_R, and the distance between the roll axis and the center of gravity of the sprung

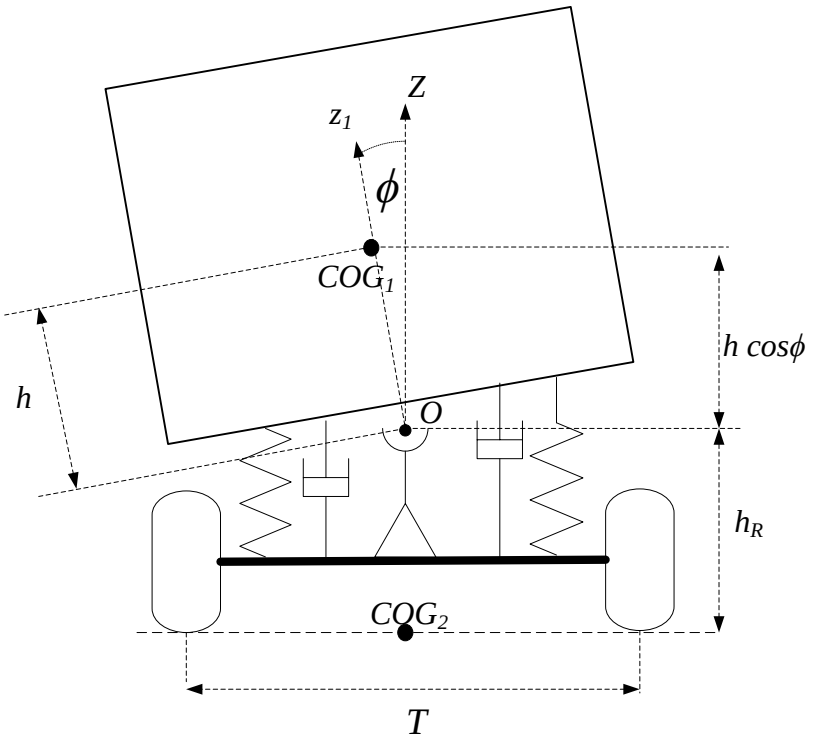

Figure 3.3: Hand-derived roll model

mass is defined by h. Unlike the yaw model, the roll model has a track width of T. It is essential to include the track width of the vehicle in the roll model to be able to perform analysis on rollover risk.

As Pacejka presents in [25], a vehicle rolls about a 'roll axis' that the sprung center of mass does not lie on. The following assumptions were made to simplify the roll model as presented by Pacejka [25] to that shown in Figure 3.3:

1. The center of gravity of the unsprung mass was assumed to be in level with the ground.
2. Pacejka states that a vehicle has a front roll center (where the roll axis goes through) that could be of different altitude of that of the rear roll center. In the presented roll model it was assumed that the front and rear roll centers are of equal altitude.
3. The x axis was assumed to coincide with the roll axis of the model.
4. The sprung mass was assumed to be pivoted on the roll axis. Therefore the only degree of freedom of the roll model is the roll angle ϕ.
5. The suspension of the sprung mass was assumed to be torsional about point O. Therefore a torsional stiffness coefficient, k_ϕ, and torsional damping coefficient, $d_{\dot{\phi}}$, were used in place of the dampers and springs present at each corner of the vehicle.

6. The vehicle was assumed to have a mass moment of inertia, $I_{xx'}$ about an axis parallel to the x axis that intersects COG_1.

The roll model presented is a one degree of freedom model and therefore only one equation of motion could be extracted. The equation of motion could be evaluated by performing Euler's equation with the parallel axis theorem for the sprung mass about the x axis.

$$\sum M_O = \left(I_{xx'} + m_1 h^2\right) \alpha_x - m_1 h a_y \tag{3.7a}$$

$$m_1 g h \sin\phi - k_\phi \phi - d_{\dot{\phi}} \dot{\phi} = \left(I_{xx'} + m_1 h^2\right) \ddot{\phi} - m_1 h \left(\dot{\nu} + 2uw\right) \tag{3.7b}$$

By rearranging Equation (3.7b) to become analogous with the linear standard format of $M\ddot{\phi} + D\dot{\phi} + K\phi = F$, where F here will be in terms of $\sin\phi$ if left without linearizing.

$$\left(I_{xx'} + m_1 h^2\right) \ddot{\phi} + d_{\dot{\phi}} \dot{\phi} + k_\phi \phi = m_1 g h \sin\phi + m_1 h \left(\dot{\nu} + 2uw\right) \tag{3.8}$$

3.2 Analytical Model Simulations

As presented earlier, the pulse signal of the active steering system could be controlled through any of the signal's parameters (the pulse's frequency, amplitude and pattern). Whether controlling one of these parameters alone will be sufficient was not yet clear. It was decided that before moving forward, the possibility of maintaining the vehicle's yaw and roll stability by controlling only one parameter needs to be assessed. From a practical perspective, the parameter of the pulse signal that the active steering system could modify most easily is the frequency, irrespective of the kind of system used for the actuator.

The first set of simulations conducted in this research project was to assess whether controlling the frequency of the pulse signal of the active steering controller alone, while the two other parameters are held constant, would be sufficient to maintain the vehicle's yaw and roll stability in various driving conditions. The derived vehicle model was used in carrying out the simulations.

3.2.1 Simulation Setup

All the simulations carried out had the same driver's steering input through the variable $\delta(t)$ as shown in Figure 3.1. The driver's steering input consisted of a J-turn maneuver done over a period of 10 seconds. The steering input takes 1 second to reach 10° through a continuous sinusoidal wave. It then stays constant at 10°

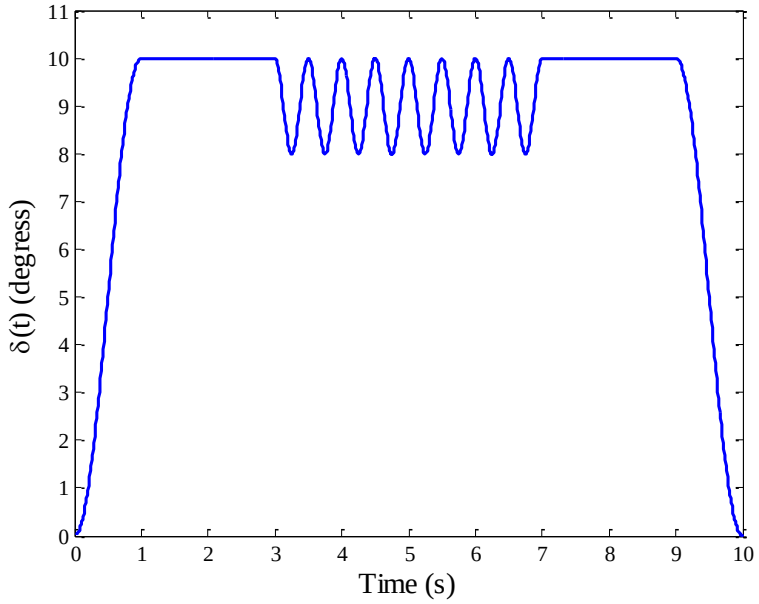

Figure 3.4: Overall steering command for simulation (2Hz Frequency)

until the 9 second mark, and then lowers to 0° in 1 second through a continuous sinusoidal wave.

The active steering controller's signal was subtracted from the driver's steering command between the 3 and 7 second marks. This is done assuming that the J-turn maneuver will cause the vehicle to be very close to rollover and therefore the active steering system was required to intervene to lower the driver's steering command. The signal throughout all simulation runs had a constant amplitude of $A = 2°$ and a symmetric pattern. The frequency however was set to 2, 4, and 8 Hz during the simulation runs to assess the effect of frequency modulation. Figure 3.4 shows the overall steering command with the 2 Hz frequency active steering pulse signal as an example. The vehicle's speed was held constant at 36 km/h (10 m/s) in all simulation runs.

3.2.2 Simulation Results

Frequency modulation of the active steering pulse signal will have an effect on the yaw and roll dynamics of the vehicle. The yaw and roll dynamic responses of each run need to be compared with some measuring scale to be able to assess whether they are improving or worsening with respect to the other simulation runs.

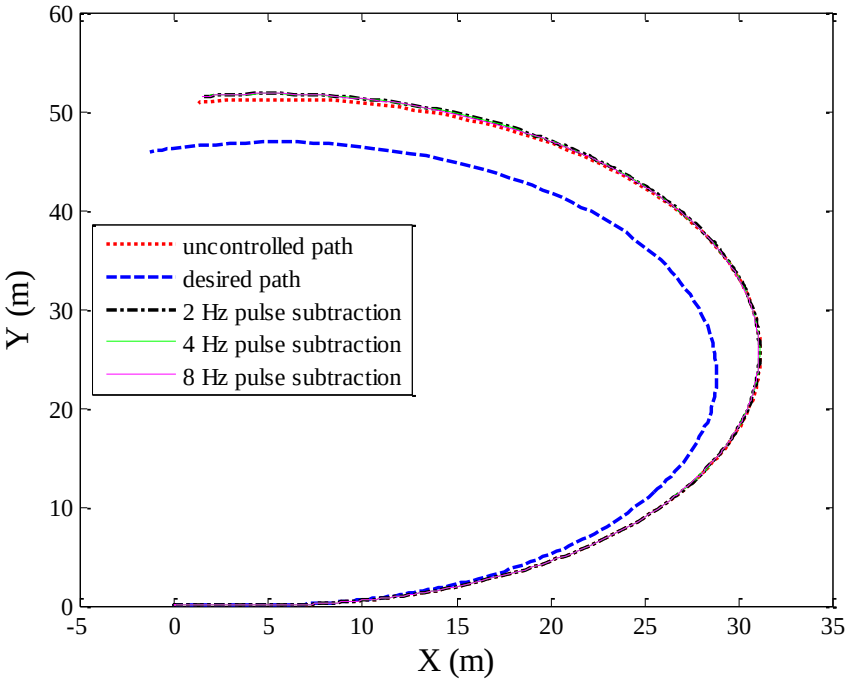

Figure 3.5: Vehicle trajectories for simulation runs compared with desire path

Yaw response

As for the measuring scale for the yaw response there are two methods found in the literature. The first method is by comparing the yaw rate responses whereas the second method is by comparing the vehicle trajectories. For both, the yaw response and the vehicle trajectory, a desired response can be evaluated through the knowledge of the vehicle's steering input, dimensions, and longitudinal velocity. The desired yaw rate could be evaluated using Equation (3.9), where w_d is the desired yaw rate and the other variables are as defined in Figure 3.1.

$$w_d = \frac{u \sin\left(\frac{L_f}{L_f + L_r}\delta\right)}{L_f \cos\delta} \tag{3.9}$$

The desired vehicle trajectory could be evaluated using Equation (3.10), where X_d and Y_d are the vehicle's desired x and y location at time t. To plot the vehicle trajectory, X_d and Y_d need to be evaluated at all time t in the range $[0, t]$.

$$X_d(t) = \int_0^t u(t) \cos\left(\int_0^t w_d(t)dt\right) dt \tag{3.10a}$$

$$Y_d(t) = \int_0^t u(t) \sin\left(\int_0^t w_d(t)dt\right) dt \tag{3.10b}$$

The yaw response of these simulation runs will be compared by the vehicle trajectories with respect to the desired vehicle trajectory. Figure 3.5 shows a plot of the vehicle trajectories of all simulation runs compared with the desired vehicle trajectory. The vehicle trajectories show that, firstly, by subtracting the active steering signal from the driver's command the vehicle's path will deviate slightly more from the desired path as compared with the uncontrolled vehicle's path. Secondly, for all frequencies used, the controlled vehicle paths were the same. This shows that there is no difference between using different frequency pulses to have an effect on the yaw dynamics of the vehicle.

Roll Response

The roll response of vehicle maneuvers are usually assessed by the rollover coefficient. The rollover coefficient, R, is considered to be an indication of whether the vehicle model would roll over. R has a range of [-1,1], when R reaches either limits this indicates that one side of the vehicle model, right or left, has lost contact with the ground, i.e. the start of a rollover. The rollover coefficient, as defined in [8], is evaluated by Equation (3.11), where the variables are as defined in Figures 3.1 and 3.3 .

$$R = \frac{2m_1}{(m_1 + m_2)T}\left((h_R + h\cos\phi)\frac{\dot{\nu} + uw - h\ddot{\phi}}{g} + h\sin\phi\right) \tag{3.11}$$

Figure 3.6 shows a plot of the rollover coefficients for the same simulation runs whereas Figure 3.7 shows a closeup. The plot shows that the local maximums of R decrease with an increase in the pulse signal's frequency. The local maximums are lowered greatly when changing from a 2Hz to a 4Hz pulse signal. However, the amount that the rollover coefficient is lowered is very minor when comparing the results of the 4Hz and 8Hz pulse signals. This shows that the rollover coefficient can be lowered through pulse frequency modulation but to a certain extent where it approaches a lower limit.

The overall results of these set of simulation runs show that pulse frequency modulation could decrease the rollover coefficient but at the same time will deviate more from the desired vehicle's path. By increasing the pulse's frequency the rollover coefficient is lowered but the vehicle trajectory will not change as compared to lower frequency pulse signal simulation runs. Finally the results show that the rollover coefficient can only be lowered to a certain limit as the pulse signal frequency increases.

In conclusion, the results show that frequency modulation has an effect on the roll and yaw dynamics, although it has a higher effect on the roll dynamics than on the yaw dynamics. This effect is limited and is not reliable to depend upon to prevent vehicle instabilities during various driving conditions.

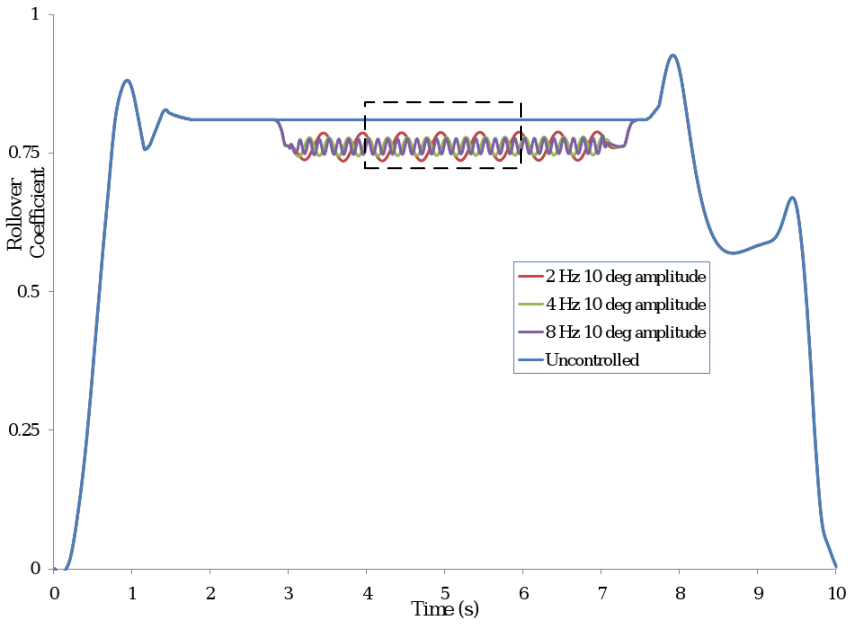

Figure 3.6: Rollover coefficient

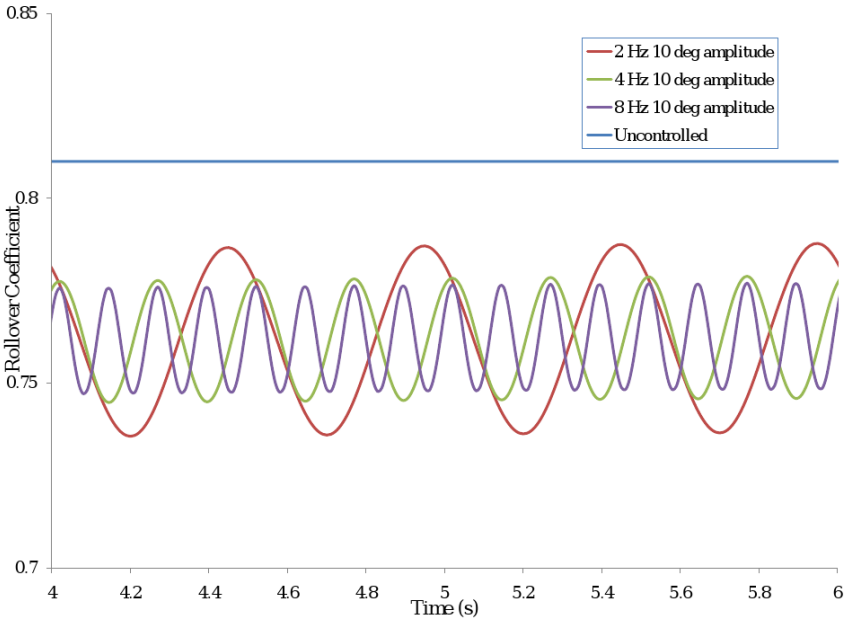

Figure 3.7: Closeup of rollover coefficient plot

3.3 DynaFlexPro Vehicle Model

In this model, DynaFlexPro was used to build a passenger vehicle having dimensional and inertial parameters comparable to Sport Utility Vehicles (SUVs). The ModelBuilder was used to generate a mathematical representation of the vehicle

model which was later exported to be used in a Matlab/Simulink environment. A simple diagram of the model is shown in Figure 3.8 with its corresponding inertial and dimensional parameters shown in section A.1, in Tables A.1 and A.2 respectively.

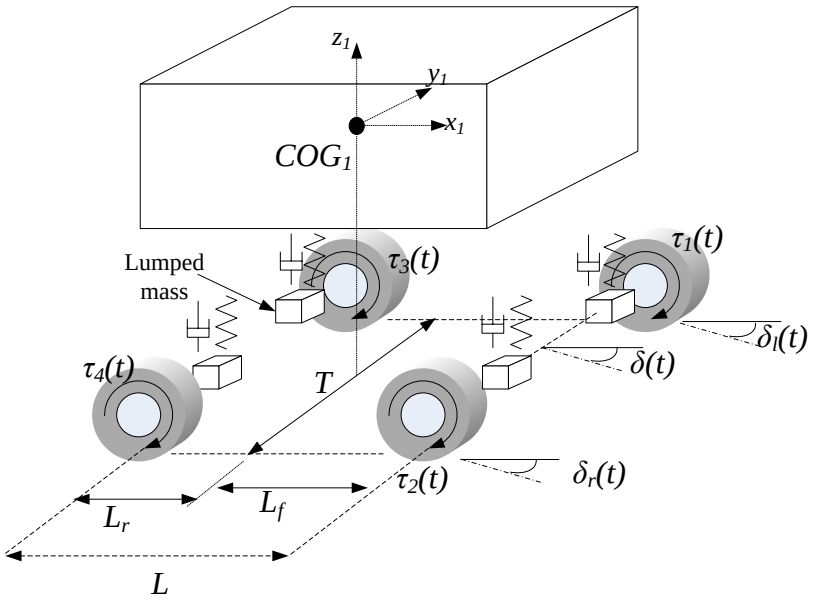

Figure 3.8: DynaFlexPro Vehicle Model

As mentioned previously, the coordinate frame (x_1, y_1, z_1) is considered to be the body-fixed frame of the sprung mass. The unsprung mass is represented by a lumped mass in addition to the tires' mass at each of the vehicle's corners. L is the distance from the front-axle to the rear-axle. The steering input(s) to the vehicle, $\delta_r(t)$ and $\delta_l(t)$, are the front right and left tires' steering angles respectively, though $\delta_r(t)$ and $\delta_l(t)$ are related through the consideration of the Ackermann's angle. The stiffness and damping constants for the springs and dampers of the vehicle model are presented in Table A.2. The wheels torques, $\tau_{1-4}(t)$, are applied independently to each tire. The tire model used in the vehicle model is the Pacejka2002 model provided in DynaFlexPro. Tire parameters used are described in detail in [21].

The sprung mass of this model has a full 6 degrees of freedom (DOF), in addition each tire has one degree of freedom as well as the suspension at each corner of the vehicle. The two front tires have another degree of freedom that allows them to steer the vehicle. Therefore the vehicle has a total of 14 DOF . The code generated was based on the model having 36 states, and 6 inputs. The 36 states with their respective initial conditions are mentioned in section A.1 in Table A.3. The inputs to the model are the wheel torques, $\tau_{1-4}(t)$, and the steering inputs, $\delta_r(t)$ and $\delta_l(t)$ as shown in Figure 3.8.

3.4 DynaFlexPro Vehicle Model Simulations

The group of simulations presented in section 3.1 showed that controlling the pulse's frequency alone was not sufficient to insure the vehicle's roll and yaw stability. The next step was to know the effect each of the pulse's parameters has on the vehicle's roll and yaw response. The results that were obtained should be sufficient to design a controller for the active safety system such that yaw and roll stability are ensured for various driving conditions.

To be able to assess the actual effect of each of the pulse's parameters, it is important to look in parallel at the yaw and roll dynamic response of the model for each simulation run carried out. The following subsections will present the conditions and assumption that were made for all simulation runs.

3.4.1 Driver's Steering Input

All simulations carried out on the DynaFlexPro vehicle model had the same driver's steering input. The steering input was through the input variable $\delta(t)$ as shown in Figure 3.8. The variable $\delta(t)$ represents the steering angle at the mid front-axle location. The vehicle model had the steering inputs divided into front right and left angles, but Ackermann's angle was taken into consideration to evaluate the right and left front tires' steering angles, $\delta_r(t)$ and $\delta_l(t)$ respectively, from $\delta(t)$. Accounting for Ackermann's angle would cause the results obtained to be more reliable. It is possible to show by geometry that $\delta_r(t)$ and $\delta_l(t)$ can be evaluated as follows when the turning circle centre is located to the right of the vehicle, i.e. vehicle is turning about $-z_1$.

$$\delta_r\left(t\right) = \tan^{-1}\left(\frac{L}{W\left(t\right)}\right) \tag{3.12a}$$

$$\delta_l\left(t\right) = \tan^{-1}\left(\frac{L}{T + W\left(t\right)}\right) \tag{3.12b}$$

$$W(t) = \frac{L}{\tan\delta\left(t\right)} - \frac{T}{2} \tag{3.12c}$$

Equations (3.12a) and (3.12b) interchange for $\delta_l(t)$ and $\delta_r(t)$ respectively when the turning circle center is located to the left of the vehicle, i.e. vehicle is turning about z_1. As presented in Equation (3.12c), a singularity is encountered in evaluating the right and left steering angles from $\delta(t)$. To overcome the problems that the singularity will generate during simulations, curve fitting was considered to evaluate the right and left steering angles. Equation (3.13) shows a fourth degree polynomial curve fitted equation with a norm of residuals less than 0.05 that was formed to present $\delta_l(t)$ and $\delta_r(t)$ in terms of $\delta(t)$.

$$\delta_l\left[\delta_r\right](t) = 1.022\delta + [-]0.2576\delta^2 - 3.422 \times 10^{-3}\delta^3 - [+]0.06777\delta^4 \tag{3.13}$$

To achieve results that allow for reliable conclusions to be extracted, it is important to have a degree of consistency in all simulations. That is why the same steering input, that represents the driver's steering command, was used throughout all simulations. The steering command of the driver, as shown in Figure 3.9, represents a J-turn maneuver of the vehicle. The J-turn is a common maneuver that is used readily in assessing the roll stability of passenger vehicles [22].

The maneuver starts after 4 seconds of simulation time, this is to allow for the vehicle model to settle from any transients present due to its initial conditions. The steering input then rises in 1 second to 10.5° in a sinusoidal shaped wave and stays constant at 10.5° for 4 seconds. It then returns in 1 second to 0° in the same sinusoidal shaped wave pattern. The steering input is kept at 0° for 2 seconds till the simulation run ends. The J-turn maneuver is shown in Figure 3.9.

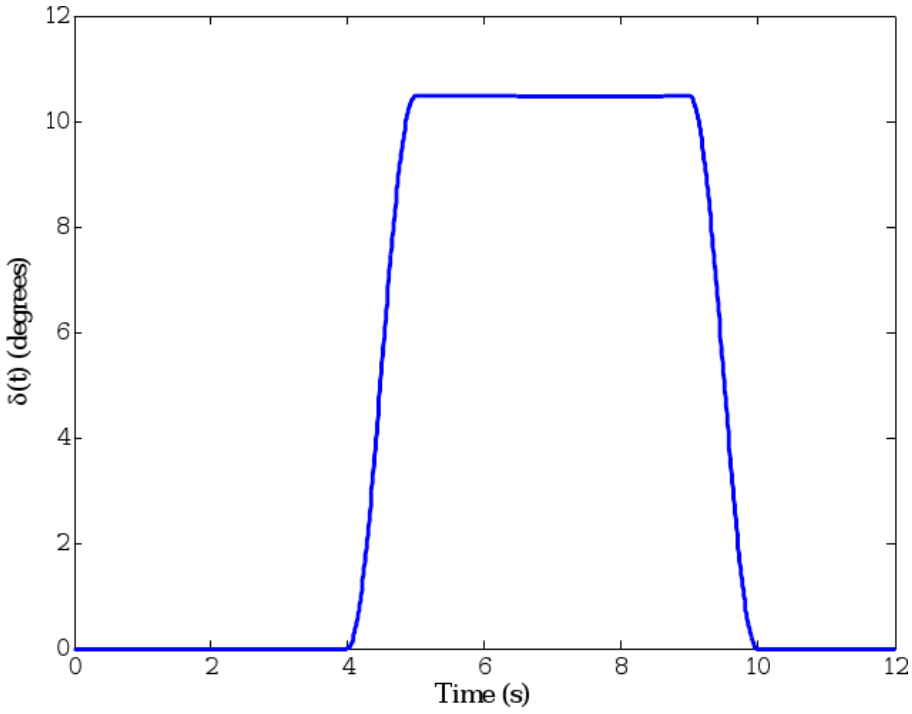

Figure 3.9: Driver's steering command

3.4.2 Longitudinal Velocity

The longitudinal velocity of the model was held constant throughout the simulations irrespective of the vehicle's dynamic state. To enable this, a control system was added to the vehicle model to control the wheel torques $\tau_{1-4}(t)$. A PID controller

was chosen to feed back the error between the actual velocity and the desired velocity. The wheel torques were allowed to have both positive and negative values, i.e. to accelerate as well as to decelerate. The torque actuated due to the velocity error signals was applied to all four wheels equally, this is shown in Figure 3.10. The desired velocity for all simulation runs was set to 20 m/s. The gains for the PID controller were chosen such that the velocity is kept in the range of ± 0.2 m/s from the desired velocity.

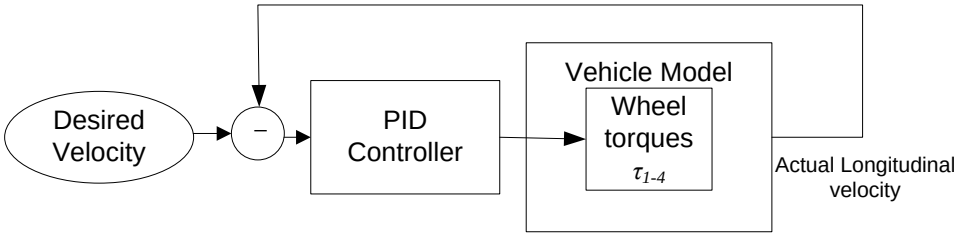

Figure 3.10: Longitudinal velocity control system

3.4.3 Procedure of Simulations

Simulations were carried out with the vehicle model performing the J-turn maneuver, as shown in Figure 3.9. A pulsed signal was used to represent the active steering controller's intervention. An initial simulation was carried out without any intervention from the controller and was found that, at the selected desired velocity, the vehicle model would be very close to rolling over between 5-9 seconds of the simulation time. It was decided therefore to fix the intervention of the active steering controller's signal between 4.5 and 9.5 seconds of the simulation time, as shown in Figure 3.11. This should not affect the validity of the conclusions that will be derived from the simulation results because it is the active steering controller's signal that is under study and not the controller design itself.

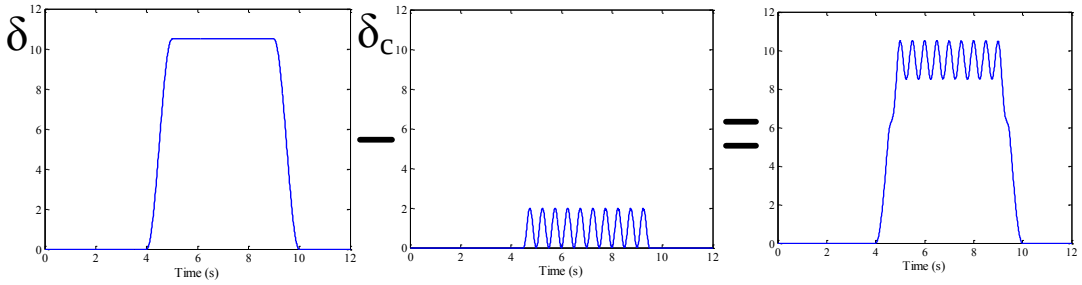

Figure 3.11: Active steering controller's intervention

To be able to assess each of the pulse parameter's impact on the yaw and roll dynamics of the vehicle model, each parameter should be assessed alone. The parameters under study consist of the amplitude, frequency and pattern of the

pulse. The simulation runs were divided into three groups. Each group consisted of fixing two of the three pulse parameters while the third parameter would be altered between simulation runs in the group.

3.4.4 Pulsed Active Steering Signal

The equation(s) used to represent the pulse signal in the simulations should be flexible to change any of its parameters outlined previously. There were two kinds of pulses that were used in the simulations; a symmetric pulse and an asymmetric pulse. A normal sinusoidal pulse was used to represent a symmetric pulse which was easy to change its frequency, and amplitude but not its pattern. Therefore the symmetric pulse was used for two group simulations; the changing amplitude group, and the changing frequency group. The asymmetric pulse was used for the changing pulse group simulations. Figure 2.5 shows plots of the symmetric and the asymmetric pulse.

In Figure 2.5, A is the amplitude and t_T is the time period of the pulse. The pattern of the asymmetric pulse can be determined through the ratio of a to b or vice versa. As for the asymmetric pulse, Equation (3.14) was used to be able to control the pattern of the pulse.

$$\delta_c(t) = \frac{A}{2}\left(1 - \cos\left(\exp\left(f\left(t_T - t\right)^n\right) - 1\right)\right) \tag{3.14}$$

Where,

$$f = \ln\left(2\pi + 1\right)\left(\frac{1}{t_T}\right)^n \tag{3.15a}$$

$$n = 0.335\left(\frac{b}{a} + 0.46\right) \tag{3.15b}$$

3.4.5 Changing Amplitude Group Simulations

In this group of simulations, the active steering control signal was set to be a symmetric pulse having a frequency of 3 Hz. The amplitude of the active steering controller's signal was changed for each simulation. Amplitudes of A= 2°, 3°, 3.5° and 4° were used for $\delta_c(t)$. To assess the roll response of the vehicle, the rollover coefficients R for all simulation runs were recorded and compared. As for the yaw response, the actual yaw rate for all simulations were recorded and compared with the desired yaw rate response.

Figure 3.12 shows a plot of the rollover coefficients recorded throughout all simulation runs whereas Figure 3.13 shows a closeup. The results show that increasing the pulse amplitude A lowers the local maximums of the rollover coefficient R of the simulation.

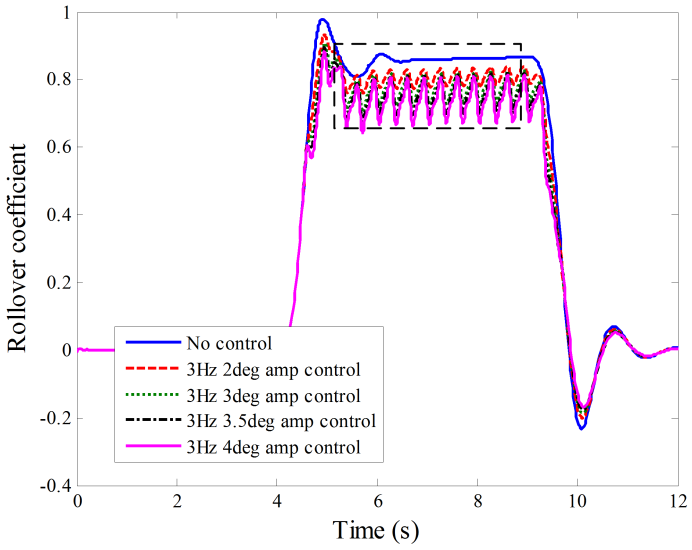

Figure 3.12: Rollover coefficients plots for changing amplitude simulations

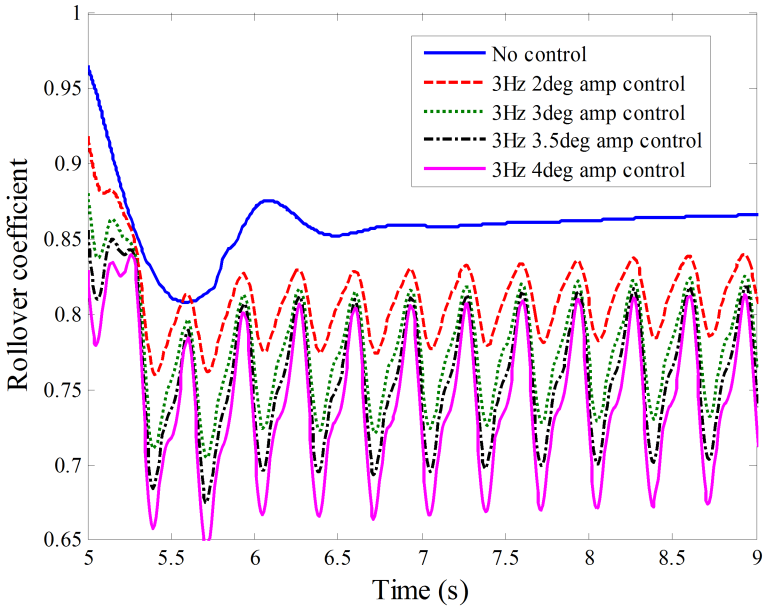

Figure 3.13: Closeup of rollover coefficients plots

The actual yaw rate response of the vehicle, as shown in Figure 3.14, deviates from the desired yaw rate as A increases. This would cause the vehicle to deviate further away from the desired path trajectory than that of the uncontrolled vehicle trajectory as the pulse amplitude A increases. The vehicle trajectory plot is presented in Figure 3.15.

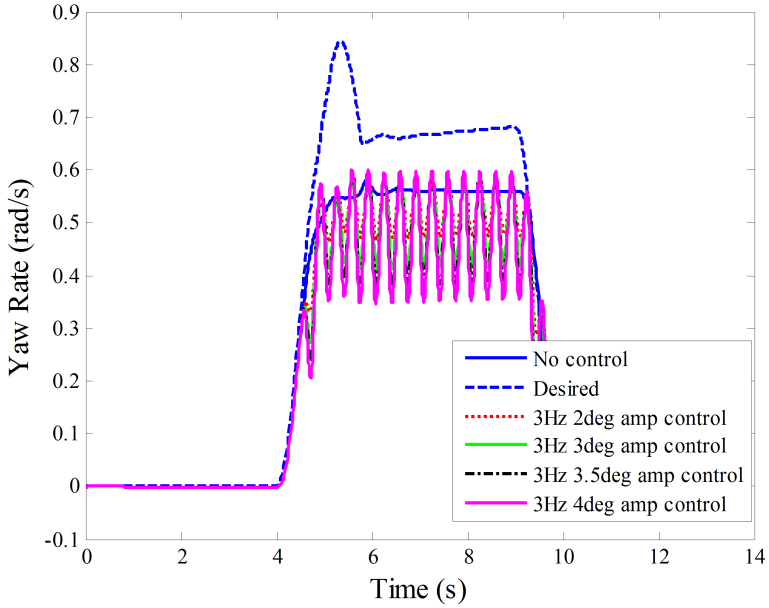

Figure 3.14: Yaw rates plot for changing amplitude simulations

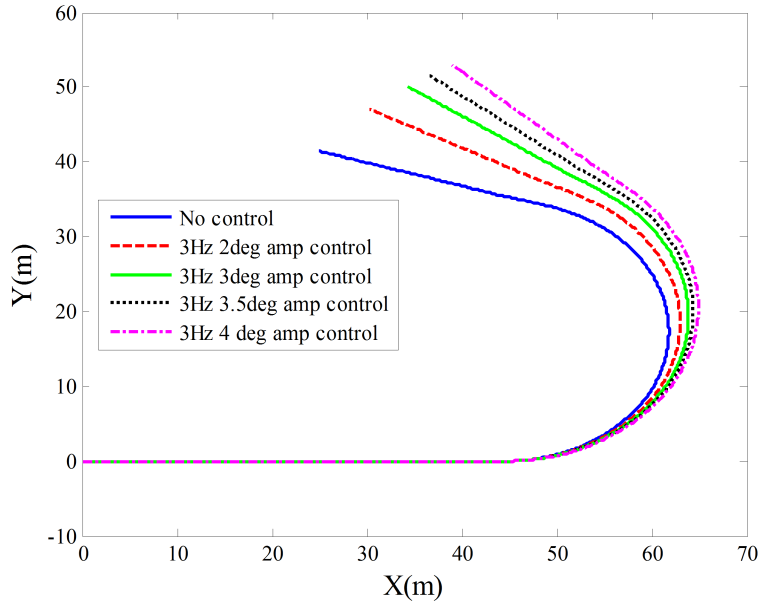

Figure 3.15: Vehicle trajectory for changing amplitude simulations

3.4.6 Changing Frequency Group Simulations

All simulations in this group had the active steering control signal, $\delta_c(t)$, set to be symmetric with an amplitude of $A = 3°$. The frequencies were changed between simulation runs to cover the frequencies of 1, 2, 3, 4, and 8Hz. A plot of the rollover

coefficients recorded for all simulation runs is shown in Figure 3.16, whereas Figure 3.17 shows a closeup.

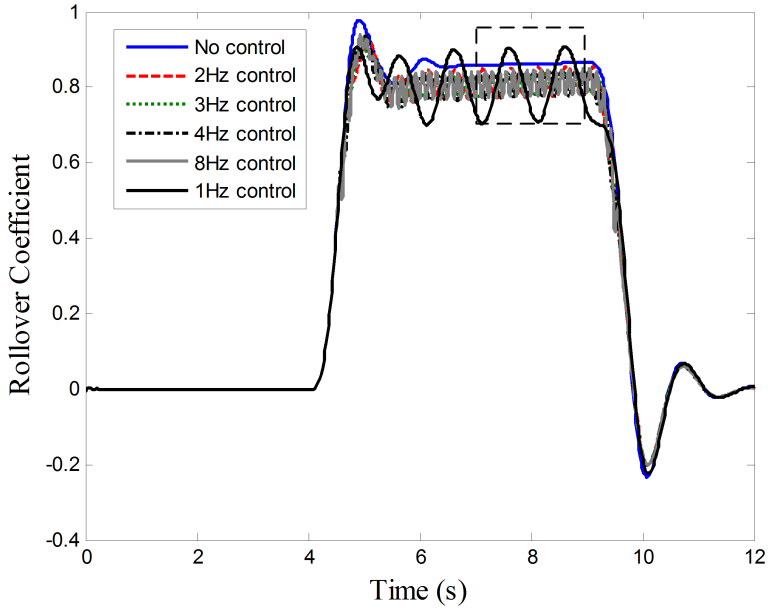

Figure 3.16: Rollover coefficients plot for changing frequency simulations

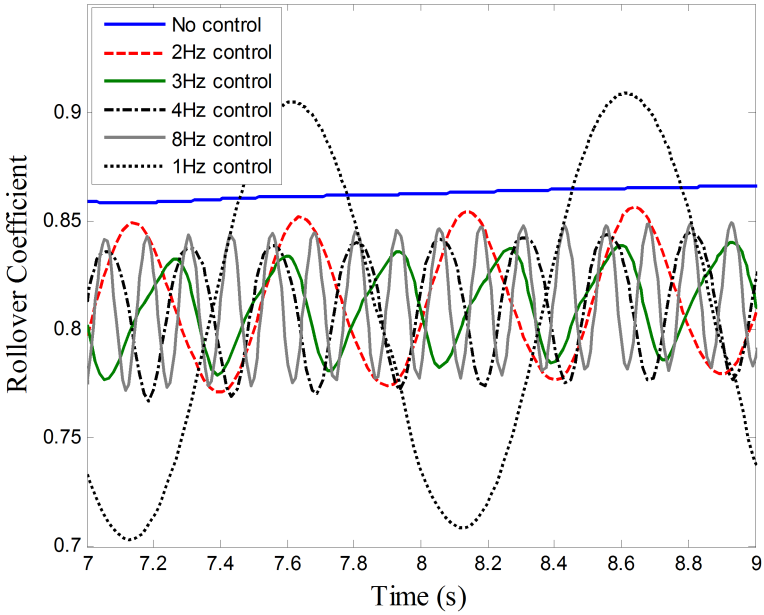

Figure 3.17: Closeup of rollover coefficients plot

The frequency of the pulse does have an impact on the vehicle's roll dynamics though its impact is less than that of the pulse's amplitude. The results depicted in

Figure 3.17 show that the rollover coefficient in the 1Hz pulse simulation increased even more than the rollover coefficient in the uncontrolled simulation run.

However, it is interesting to note that the first roll natural frequency of the vehicle model used was 2.7Hz; this is evaluated from the data shown in Appendix A.1. By having a closer look at the results, with the aid of Figure 3.17, it is clear that the simulation run containing the 3Hz frequency pulse had the lowest local maximums amongst all the other simulation runs. This insight strongly supports that by setting the frequency of the active steering pulse equal to the vehicle's roll natural frequency will lower the risk of a rollover the most, i.e. lower the rollover coefficient.

By setting the pulsed active steering signal to have a frequency equal to the roll natural frequency we are adding a harmonic force having the roll natural frequency in the lateral direction. This will cause the vehicle to vibrate at resonance away from the vehicle side in danger of rolling over.

As for the yaw response of the vehicle with respect to changing the frequency of the pulse, results show that the frequency has no effect on the yaw response. Figure 3.18 shows a plot of the actual yaw rates of the simulation runs as well as the desired yaw rate response whereas Figure 3.19 shows a closeup. The yaw rate response for different frequencies average out to be approximately the same. This could be seen clearly through the vehicle trajectory plot in Figure 3.20, where all simulation runs show that the vehicle took the same trajectory.

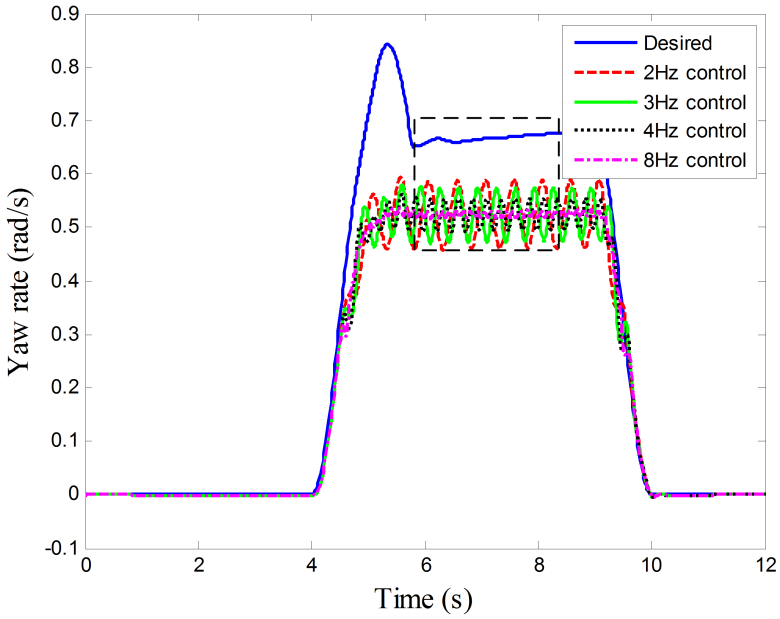

Figure 3.18: Yaw rate response plot for changing frequency simulations

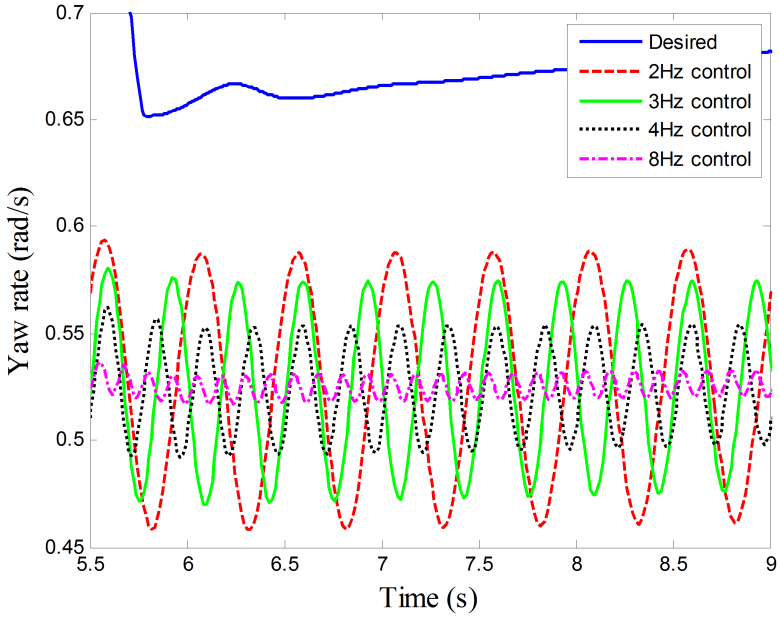

Figure 3.19: Closeup of yaw rate response plot

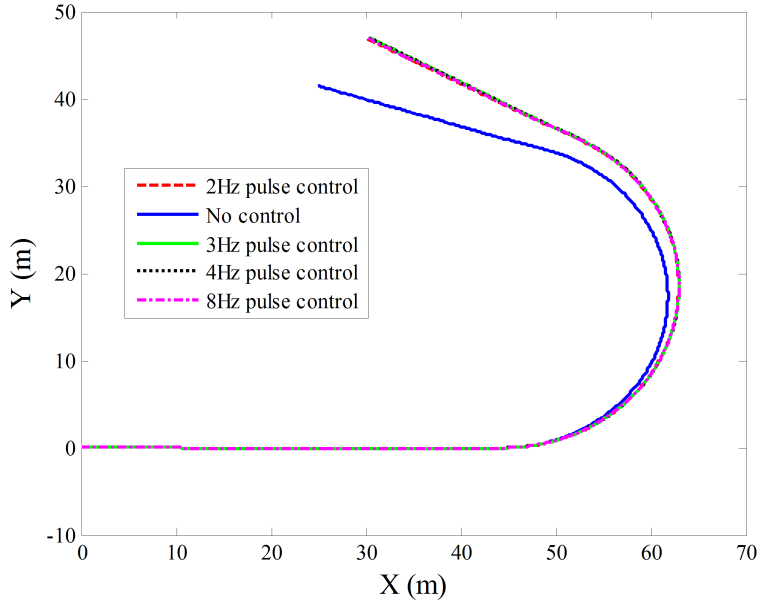

Figure 3.20: Vehicle trajectory for changing frequency simulations

3.4.7 Changing Pulse Pattern Group Simulations

This group of simulations consisted of using the pulsed active steering signal with different pulse patterns with fixed amplitude and frequency throughout. All pulse patterns assessed were fixed at a frequency of 3Hz and an amplitude of $A = 3°$. The

pulse patterns assessed consisted of symmetric and asymmetric shaped pulses. The asymmetric shaped pulses were defined based on the ratio b/a as shown in Figure 2.5. Asymmetric pulses used had ratios b/a= 0.56, 0.77, 1.3, and 1.8. Figure 3.21 shows the plots of the rollover coefficients for the group's simulations, whereas Figure 3.22 shows a closeup.

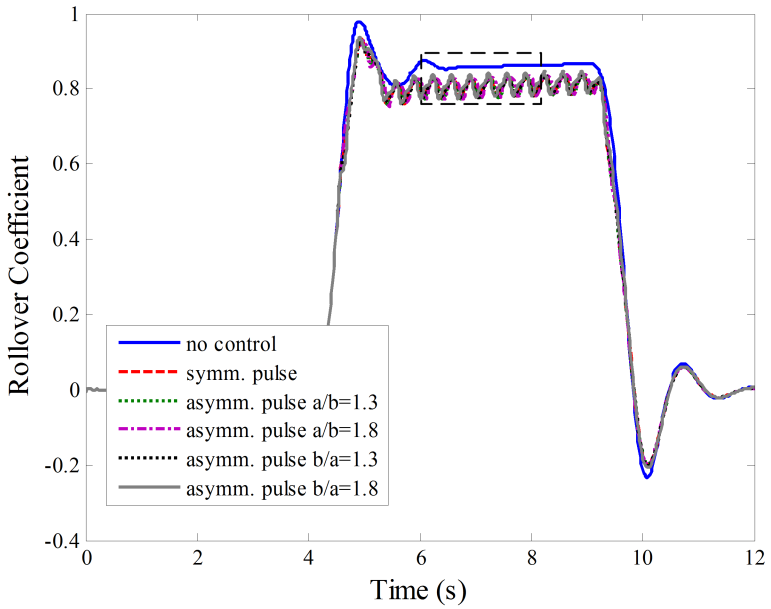

Figure 3.21: Rollover coefficients plot for changing pulse pattern simulations

As shown in Figure 3.21, pulse patterns having an a/b ratio less than 1 had higher rollover coefficient local maximums as compared to pulse patterns having an a/b ratio more than 1. The pulse pattern that resulted in obtaining the lowest local maximums of R was the $a/b = 1.3$ pulse pattern. It cannot be concluded though that the $b/a = 0.56$ pulse pattern gives the optimal vehicle response until the yaw response is assessed in parallel with Figure 3.21.

The vehicle trajectories for the same simulation runs are shown in Figure 3.23. For the J-turn maneuver used throughout this section's simulations, it is preferable that the rollover of the vehicle is prevented with as minimal as possible vehicle trajectory deviation from the uncontrolled path (or from the desired path). Figure 3.24 shows that the pulse patterns of $b/a = 1.8$ and $a/b = 1.8$ are slightly closer to the uncontrolled vehicle trajectory when compared to the other pulse patterns used. The symmetric pulse had the next lowest trajectory deviation followed by the pulse patterns $b/a = 1.3$ and $a/b = 1.3$. Therefore the results presented show that the pulse pattern that gives the most preferable compromise between the roll and yaw dynamics of the vehicle is the $a/b = 1.8$ pulse pattern. The $a/b = 1.8$ pulse pattern gave the least path deviation and as well, gave the second lowest rollover coefficient local maximums (next to the $a/b = 1.3$ pattern).

Only a few pulse patterns were used in the pulse pattern simulation group runs,

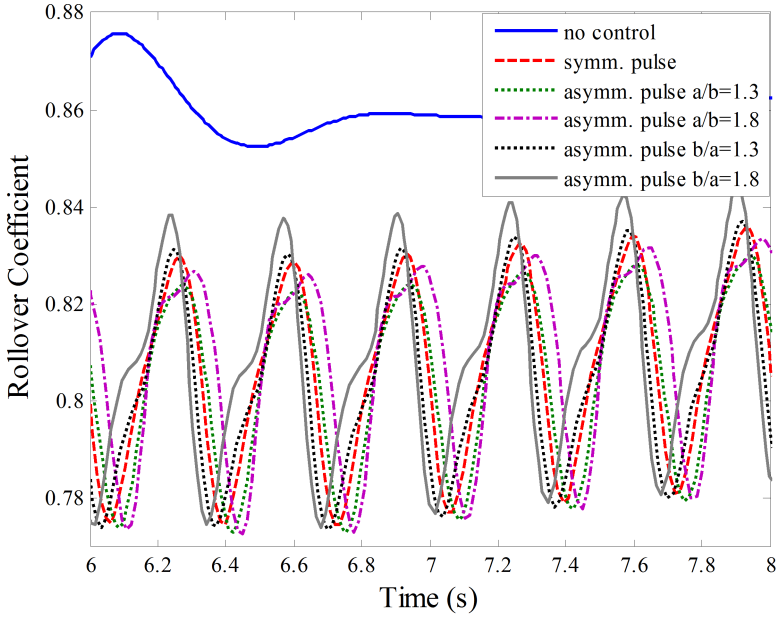

Figure 3.22: Closeup of rollover coefficient plot

and therefore it can not be strictly concluded that the $a/b = 1.8$ pulse pattern will give the best vehicle response out of all other possible pulse patterns. To assess this further, an optimization study will be required to minimize an objective function that will incorporate the yaw and roll dynamics of the vehicle. This will be considered as future work with respect to this research project.

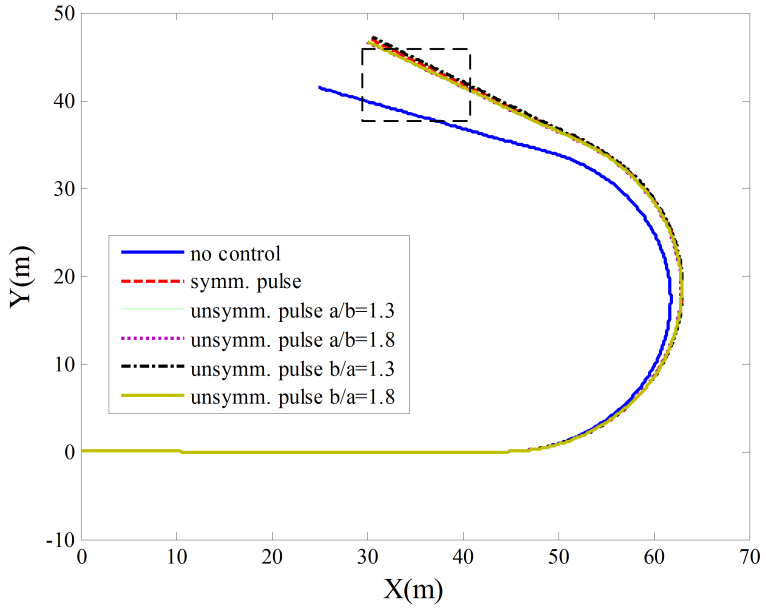

Figure 3.23: Vehicle trajectory plots for changing pulse pattern simulations

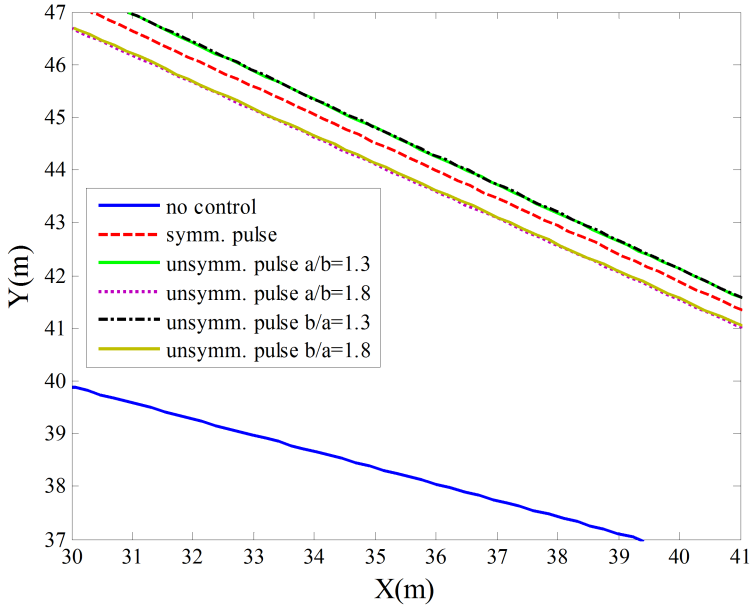

Figure 3.24: Closeup of vehicle trajectory plot

3.5 Adams/Car Model

The DynaFlexPro vehicle model simulation results showed the effect each pulse parameter has on the yaw and roll dynamics of the vehicle. The objective of this set of simulations was to obtain numeric values associated with the steering system. This would assist in the design of the potential experiment of this research project.

Adams/Car was a suitable platform to achieve this objective. Adams/Car enables you to track the dynamics of any part of the vehicle model, which includes the steering system. All the simulations were made using the non-linear demonstration vehicle model provided by Adams/Car. The tire-model used was the Pacejka 2002 tire model, which consists of the Magic Formula for both longitudinal and lateral tire forces. The Pacejka 2002 tire model also includes the transient response to friction changes as well as the slip dependent relaxation effect. Parameters of the demonstration vehicle model are shown in Table A.4.

In designing the potential experiment, there are some numeric values associated with the steering system that needs to be known. Such values include the steering wheel equivalent moment of inertia and the amount of torque assist that is supplied to the driver from the power steering system. These numeric values will help in sizing the potential experiment components. Each of the following subsections will present how each of these values were obtained.

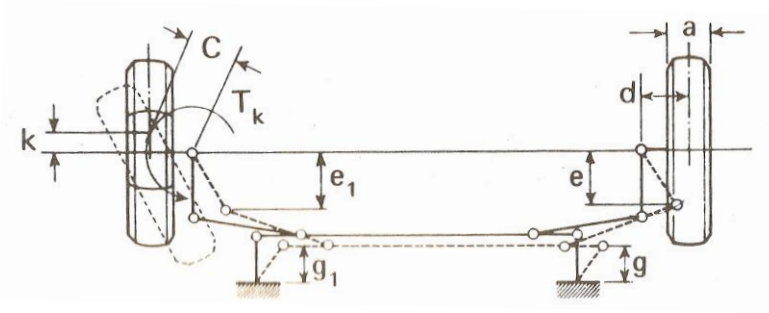

Figure 3.25: Definition of geometric variables of a steering system [11]

3.5.1 Steering Wheel Inertia

When turning a steering wheel, the driver feels a resistive torque to his motion, which is due to the self-aligning torque applied on the front wheels while turning. This resistive torque can be approximated, with a good degree of accuracy, to be treated as the moment of inertia of the steering wheel. Evaluating the steering wheel's mass moment of inertia will be beneficial to know the amount of torque that will be required to cause a certain angular motion, whether it is from the driver or the active steering controller. The first consideration to evaluate the steering wheel inertia was through the knowledge of the front wheels' self-aligning torque. The direct relation between the steering wheel torque and the front tires' self-aligning torque is presented in Equation (3.16).

$$T_{sw} = T_k \frac{\frac{g_1}{e_1} + \frac{g}{e}}{S_R \eta_b} \tag{3.16}$$

Where T_{sw} is the steering wheel torque and T_k is the kingpin torque, which is the same magnitude as the self-aligning torque. S_R is the steering ratio of the vehicle and η_b is the efficiency of the gear connection between the steering column and the steering rack. The values g_1, e_1, g, and e are geometric variables of the steering system as presented in Figure 3.25 [11].

The geometric variables of the steering system change during turning and therefore it was difficult to gain the steering wheel torque through the knowledge of the self-aligning torque. The second consideration to evaluate the steering wheel inertia was through the use of Adams/Car. Adams/Car is capable of recording the steering column torque, which then can be used alongside Euler's simplified equation (3.17) to evaluate the steering wheel's moment of inertia.

$$T_{sw} = I_{sw} \alpha_{\delta_t} \tag{3.17}$$

In Equation (3.17), T and I with the subscript sw represent the steering wheel's applied torque and mass moment of inertia respectively. α_{δ_t} represents the angular acceleration of the total steering input. Therefore the variables that are of interest

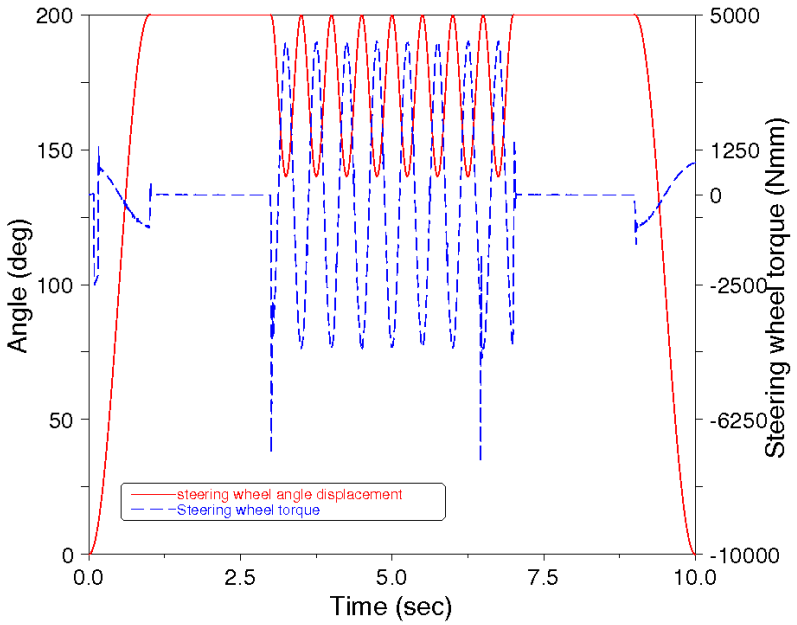

Figure 3.26: Overall steering input with corresponding steering wheel torque for pulse of 2Hz

that need to be recorded in these simulation runs are only the steering wheel input, which will be used to evaluate α_δ, and the steering column or wheel torque. It was decided that a steering input of a J-turn maneuver with the active steering symmetric pulse subtraction will be used in these simulations. The first simulation run included an active steering pulse with an amplitude of 60°, at the steering wheel level, and a frequency of 2Hz. The overall steering command with it's respective steering wheel torque recorded from the simulation run are plotted in Figure 3.26.

Figure 3.26 shows that during the periods where the overall steering command is constant and nonzero (1-3 sec and 7-9 sec), the steering wheel torque is zero. This contradicts with what actually happens, where if there is no torque applied to the steering wheel from the drivers side, the steering angle will slowly return to zero due to the resistive torque that was mentioned earlier. What Adams/Car actually does, most likely due to how the vehicle demo model was built, is that it considers the torque applied from the driver's side to maintain the steering angle as part of the power steering torque assist rather than part of the steering wheel torque applied by the driver. But this will not affect the study done here. During the subtraction of the pulse steering signal, the overall steering command can be evaluated using Equation (3.18).

$$\delta_t = \delta - A/2\left(1 - \cos(\frac{2\pi}{t_T}(t - t_i))\right) \tag{3.18}$$

In Equation 3.18, δ_t is the total steering command. A and t_T are the amplitude and time period of the active steering pulse respectively and t_i is the initial time of the

active steering pulse's intervention. By differentiating δ_t twice while δ is constant and the active steering pulse is subtracted (between 3-7 sec), α_{δ_t} becomes:

$$\alpha_{\delta_t} = -2A(\frac{\pi}{t_T})^2 \left(\cos(\frac{2\pi}{t_T}(t - t_i))\right) \tag{3.19}$$

α_{δ_t} magnitude becomes maximum when $\cos(\frac{2\pi}{t_T}(t - t_i))$ becomes 1 or -1, which occurs every 0.25 seconds between 3-7 seconds (for $1/t_T$=2Hz). At these instances, the steering wheel torque T_{sw} is also at its maximum magnitude, which from Figure 3.26 equals 4.2 $N.m$. By substituting in Equation 3.17,

$$\begin{aligned} I_{sw} &= \frac{|(T_{sw})_{max}|}{|(\alpha_{\delta_t})_{max}|} \\ I_{sw} &= \frac{4.2}{\left(2\frac{60\pi}{180}(2\pi)^2\right)} \end{aligned}$$

Therefore,

$$I_{sw} = 0.0508 kg.m^2$$

The first simulation results show that the steering wheel mass moment of inertia can be approximated to 0.05 $kg.m^2$. To assess whether this mass moment of inertia would change depending upon the steering input, a second simulation was carried out with a different pulse frequency of 4Hz. The steering input and the steering wheel torque for the second simulation run are shown in Figure 3.27.

The maximum steering torque obtained, at $(\alpha_{\delta_t})_{max}$, had a magnitude of 16.6 $N.m$. Again by substituting in Equation 3.17,

$$\begin{aligned} I_{sw} &= \frac{|(T_{sw})_{max}|}{|(\alpha_{\delta_t})_{max}|} \\ I_{sw} &= \frac{16.6}{\left(2\frac{60\pi}{180}(4\pi)^2\right)} \end{aligned}$$

Therefore,

$$I_{sw} = 0.0502 kgm^2$$

Both simulation runs show sufficient consistency in obtaining I_{sw}.

3.5.2 Power Steering Torque Assist

There are different power steering systems available for commercial passenger vehicles. Hydraulic power steering systems were commonly used in the past, however electric power steering systems are slowly replacing them due to the latter's compact size and lower power consumption. Irrespective of the kind of power steering system, they all in general perform the same task. A power steering system assists

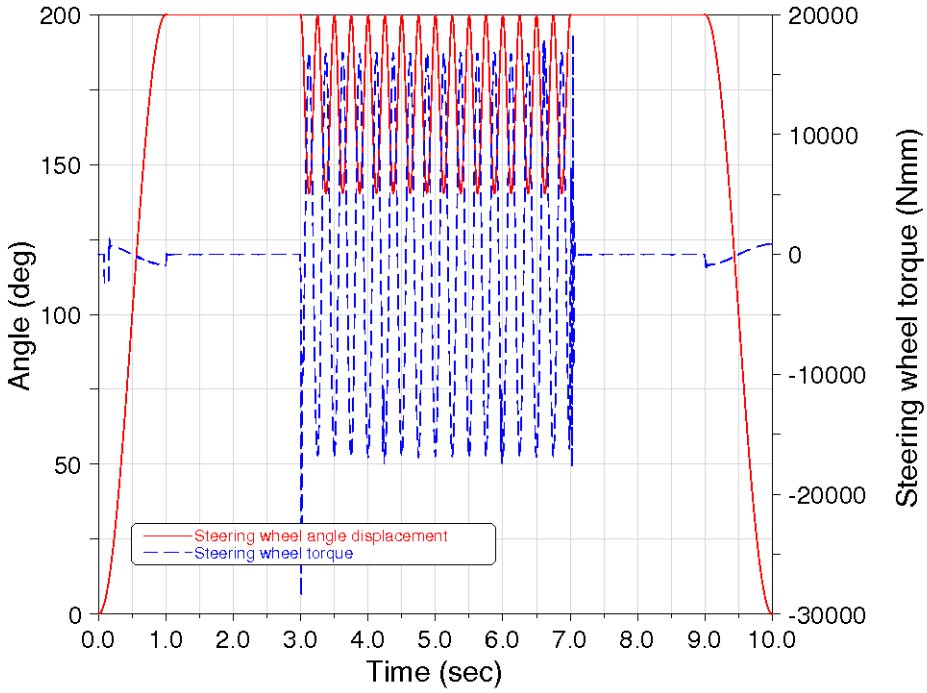

Figure 3.27: Overall steering input with corresponding steering wheel torque for pulse of 4Hz

the driver through providing a torque to lower the amount of work the driver is required to input to turn the steering wheel.

It was required to know the amount of assist the power steering system supplies with respect to various driver's steering inputs so that the components of the potential experiment can be correctly sized. The setup of the previous section's simulation runs were used for this section as well.

Adams/Car can be configured to record the power steering torque assist during a simulation run while using the demo vehicle model. The first simulation run carried out here had the same setup as the first simulation run in section 3.5.1. Figure 3.28 shows a plot of the corresponding steering assist torque.

The plot shows that the power steering torque assist had local maximums of 5.6 $N.m$ during the active steering signal intervention. Whether the torque assist would significantly increase with an increase in the active steering pulse's frequency and/or amplitude was still required to be assessed. The second simulation run carried out was to increase the active steering pulse's signal frequency from 2 to 4Hz. Figure 3.29 shows a plot of the corresponding steering assist torque.

The plot shows that the local maximums of the torque assist applied by the power steering system during the active steering intervention increased slightly to 5.8 $N.m$. This shows that an increase in the frequency of the active steering pulse would slightly increase the power steering torque assist. The following simulation

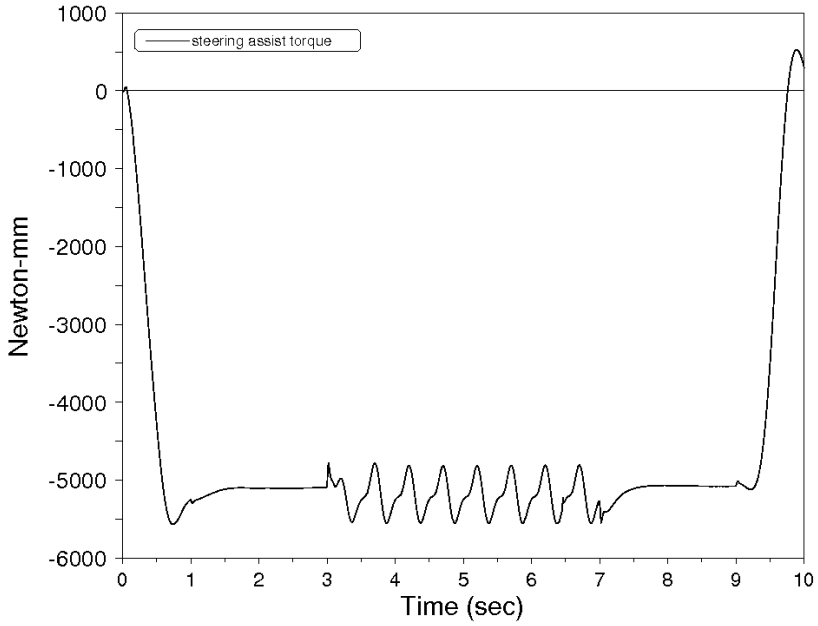

Figure 3.28: Power steering torque assist with an active steering signal of 2Hz

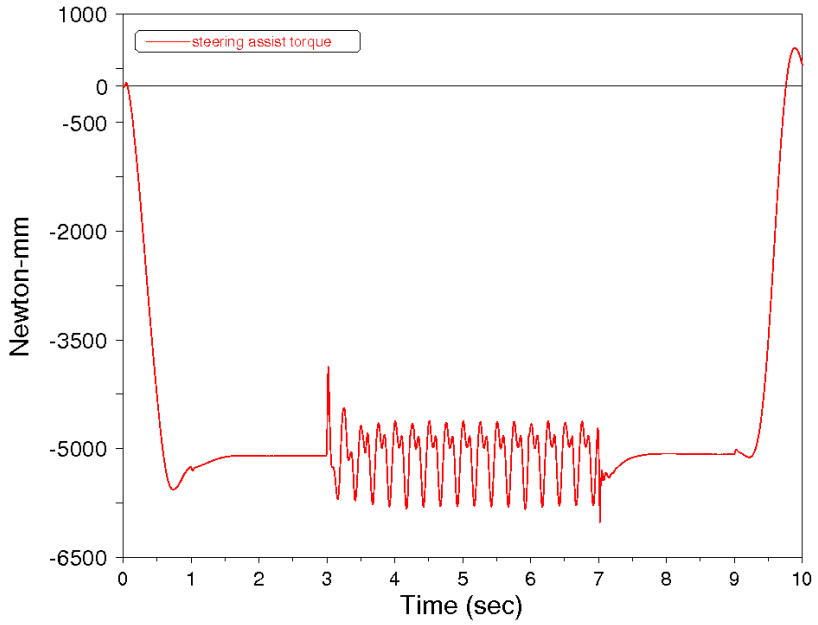

Figure 3.29: Power steering torque assist with an active steering signal of 4Hz

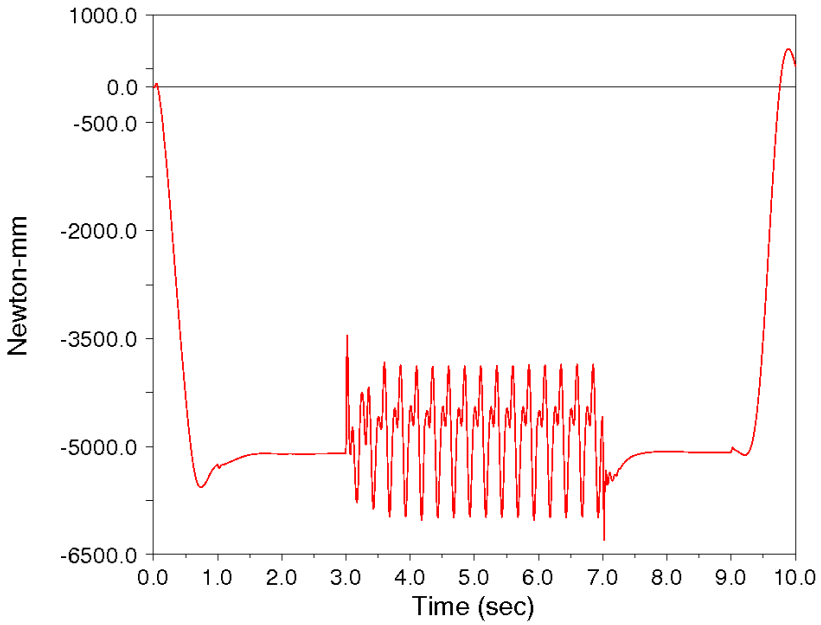

Figure 3.30: Power steering torque assist with an active steering signal of 4Hz and higher pulse amplitude

run included increasing the active steering pulse signal's amplitude from 60° to 80° as measured from the steering wheel. Figure 3.30 shows the corresponding steering assist torque.

Figure 3.30 shows that the local maximums of the torque assist applied by the power steering system during the active steering intervention were about 5.9 $N.m$. This is considered a slight increase as compared with the previous simulation run.

In conclusion, the simulation runs carried out in this section show that the power steering torque assist slightly increases with an increase in either the frequency or the amplitude of the pulse signal. However, the torque assist did not exceed 6 $N.m$, irrespective of the active steering pulse parameters chosen. Therefore it is suitable to choose 6 $N.m$ as a maximum value for the power steering torque assist when designing the potential experiment.

Chapter 4

Hardware-in-the-Loop Experiment

The simulations phase of this research project proposed conclusions that need to be verified. Verification of simulations can be done through various ways such as comparing them with benchmark results, or supporting them with analytical counterpart analysis. The method used to verify the simulation results obtained here was to compare them with experimental results. Having an experiment will not only benefit the verification of simulation results, but will also demonstrate the applicability aspect of pulsed active steering.

As shown previously in Figure 2.3, an active steering system can be attached to different parts of the steering system. For this research project, an active steering system will be designed such that it is connectable to the steering column of the vehicle's steering system, as shown in Figure 4.1. Connecting the active steering system to the steering column is considered less difficult than connecting it to the steering linkage.

This chapter will present the initial design considerations for designing an active steering system before focussing on the finalized experiment setup with its obtained results.

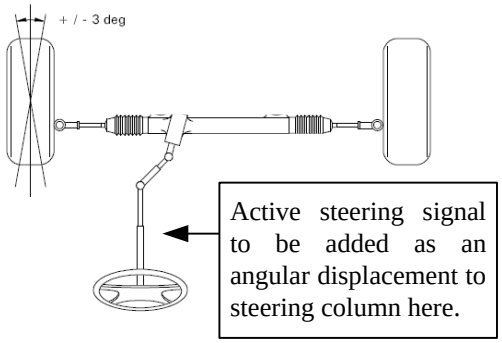

Figure 4.1: Location of active steering system to be added

4.1 Initial Considerations

Many factors need to be taken into consideration when designing an experiment for research purposes. Some factors that are not affiliated with the technical side of the research project but yet affected experimental setup considerations include cost of components, availability of components, space for experiment and the time frame in which the experiment needs to be completed.

The initial experiment designs that are listed in this section were designed prior to consideration of the non-technical factors affecting the setup. Thus some of them were ruled out due to non-technical factors whereas others were eliminated due to technical issues.

There are certain constraints that need to be satisfied in any of the proposed active steering systems. These constraints are as follows:

1. The system should allow for two angular inputs to be added/subtracted to give one angular output. This will allow adding/subtracting the active steering signal to/from the driver's steering command.
2. The system should allow the active steering pulse signal to be modulated through its amplitude, frequency, and pulse pattern.
3. The system should not under any circumstance isolate the driver input from the steering column.

There were three main initial designs that were studied thoroughly. They are: planetary gearbox, EPS system, and the differential steering system.

4.1.1 Planetary Gearbox

The first design to be considered was a planetary gearbox. A planetary gear set consists of a sun gear, a ring gear and several planet gears with their planet carrier. A planetary gearbox was designed such that the planet carrier will be used to input the driver's steering command. The ring gear will be used to add the active steering controller signal and the sun gear will be used to output the overall steering command to the steering column. This is shown in Figure 4.2.

The ring gear will be used to input the active steering signal to the steering system. Therefore a mechanism was designed to enable the control of the ring gear's angular motion. The mechanism should allow for easy control of all active steering pulse parameters (amplitude, frequency, and pulse pattern). A four-bar mechanism based design was chosen to enable the control of the ring gear's angular motion. The mechanism will be used such that the crank link is driven by a motor and the rocker is connected to the steering column through the ring gear, thus the ring gear's radius will be the rocker. But, this mechanism should be able to

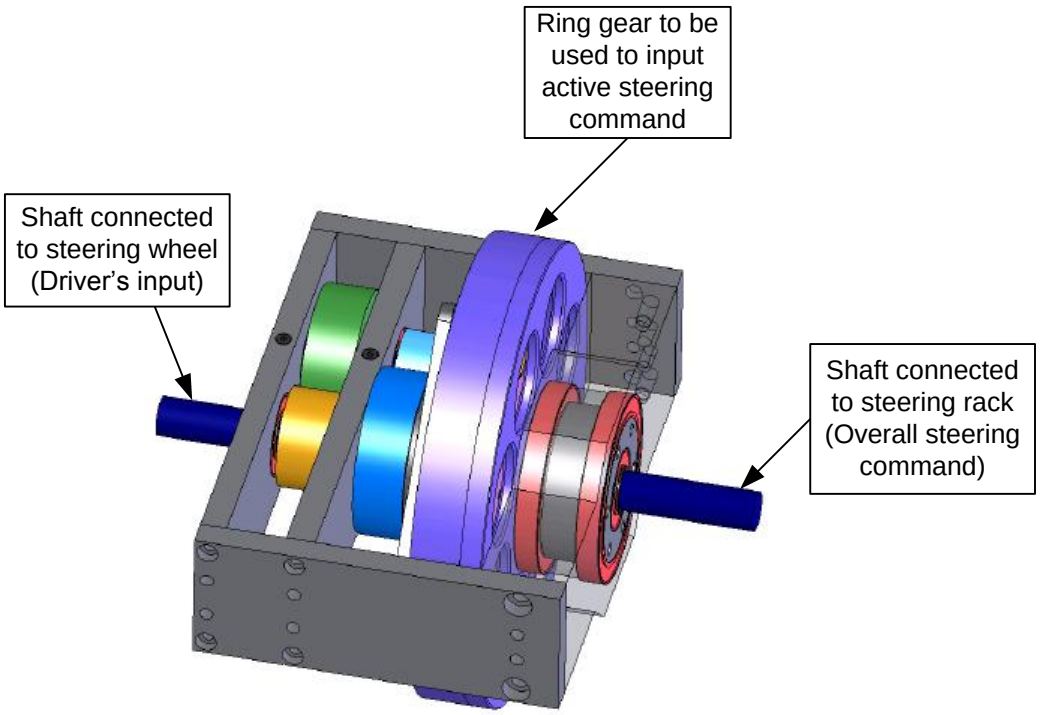

Figure 4.2: Planetary gearbox to be placed along steering column

add or subtract the desired signal to the steering command, and having only one mechanism will only either add or subtract the desired signal (changing the cranks rotation direction will just laterally reverse the desired signal).

A way to overcome this limitation is to use two mechanisms connected to one input motor. The coupler of each mechanism will be connected to a slotted curved path on the outer circumference of the ring gear through an electromagnetic switch that would act as a revolute joint when activated and as a prismatic joint when deactivated. Thus, if a situation requires the addition of the active steering signal, then the motor will be signalled to rotate in a certain direction and at the same time the electromagnetic switch will be activated at one mechanism and deactivated at the other such that the coupler of the activated mechanism will have a revolute joint whereas the coupler of the deactivated mechanism will have a prismatic joint with the ring gear. This is shown in Figure 4.3.

The active steering pulse signal parameters can be controlled through the lengths of the four bar linkage. An algorithm, shown in Appendix B.2, was constructed to evaluate these lengths based upon the required values of the pulse's amplitude, A, and pattern, b/a ratio. The frequency of the pulse can be easily controlled through the crank rotational velocity, i.e. in this case the control motor's velocity.

This planetary gearbox design option was removed from consideration due to several issues. The main issue is that the pulse signal generated will be depending upon the mechanism design parameters. Thus once the mechanism is assembled,

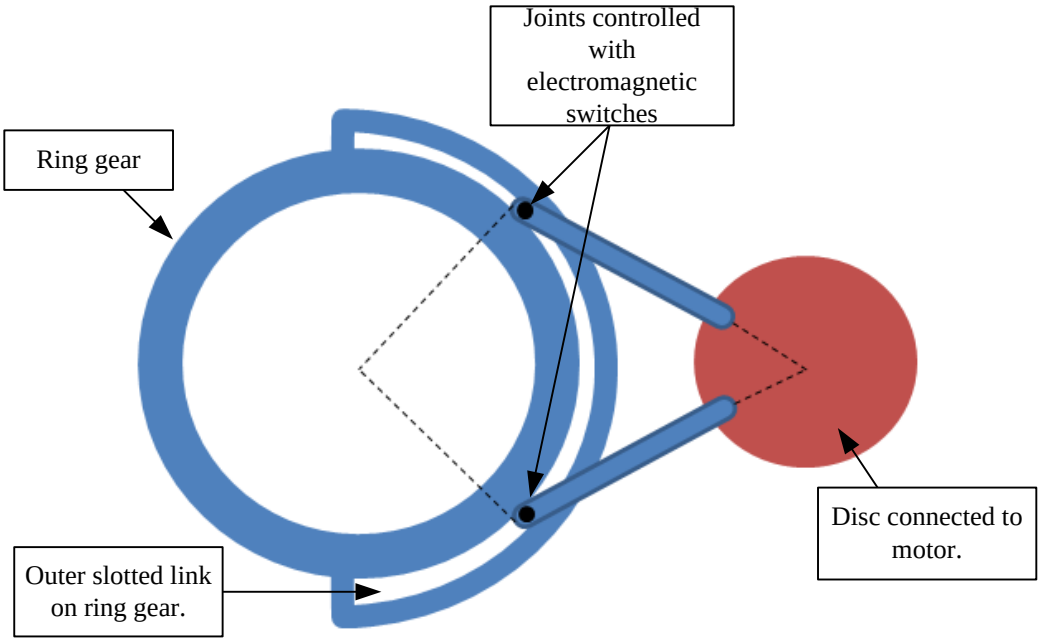

Figure 4.3: Mechanism to be connected to planetary gearbox

the pulse parameters (amplitude and pulse pattern) can not be altered unless the mechanism design parameters are changed. This will constrain the active steering system by not allowing it to choose different amplitudes and pulse patterns, if required, during different driving situations.

4.1.2 Electric Power Steering System

There are different power steering systems available for passenger vehicles. The most commonly used is the hydraulic power steering system, although it is becoming less popular due to its higher energy consumption as compared with other available systems.

An Electric Power Steering (EPS) system is a kind of power steering system that relies on electric power to assist the driver to supply the required torque to the steering system. An EPS system was considered as an option for the active steering system to be used in this experiment. To be able to do so, it was required to fully understand how the EPS functions.

An EPS system of a Chevrolet Cobalt (Figure 4.4) was obtained with its technical documentations. This EPS system uses a torque sensor, placed on the steering column, to determine the amount of steering assist required. Based on the torque sensor feedback as well as other vehicle states, the power steering control module would command the amount of power assist the control motor will provide via the motor's power amplifier. The initial idea was to isolate the torque sensor from the

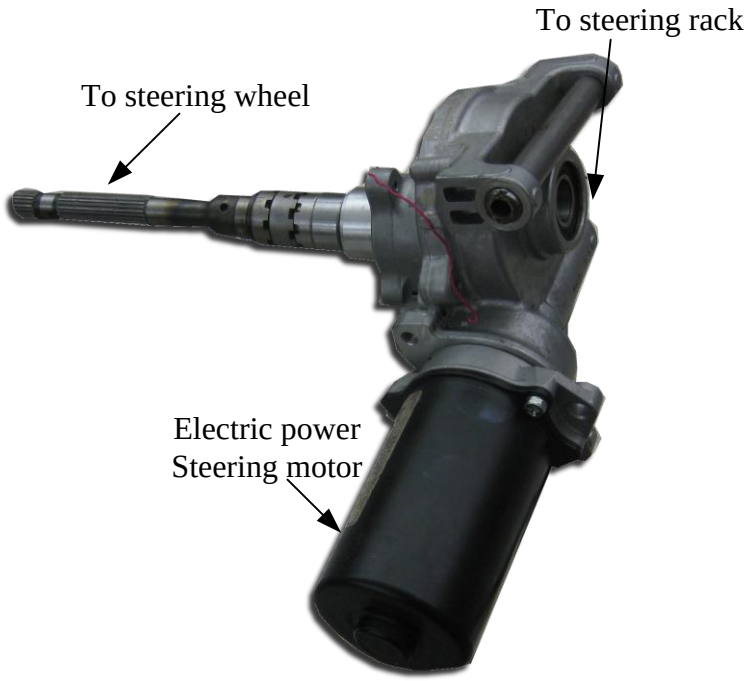

Figure 4.4: The EPS system of a 2007 Chevrolet Cobalt

system and to use its cables to send analog signals to the power steering control module and thus would be able to control the system's control motor. After several trials it was not possible to achieve this mainly because the control module also takes inputs that are coming from the Engine Computer Unit (ECU). The communication method between the ECU and other parts of the vehicle are through a General Motors (GM) proprietary method that was not readily available to us.

4.1.3 Differential

Keeping the cost of the system in mind, it was preferable to find an off-the-shell product that would satisfy the design constraints. A vehicle's differential was considered as a viable option. A differential is a mechanical device found in vehicles that transmits the torque coming from the engine to the torque driving wheels. Differentials found in passenger vehicles are generally big in size and therefore will not be appropriate for this application. A differential of an ATV (All-Train-Vehicle) was obtained from a junkyard that was considerably smaller in size and low in cost.

Differentials could be used in two different ways. The more common usage is to receive one input and provide two outputs, as found in vehicles. The other way is to combine two inputs and create an output that is the sum, difference or average of the inputs. This obtained differential can therefore be adjusted such that one input is fed by the driver while the other input is from the active steering controller. The rotational directions of the inputs will be adjusted such that the output is the combination of the two.

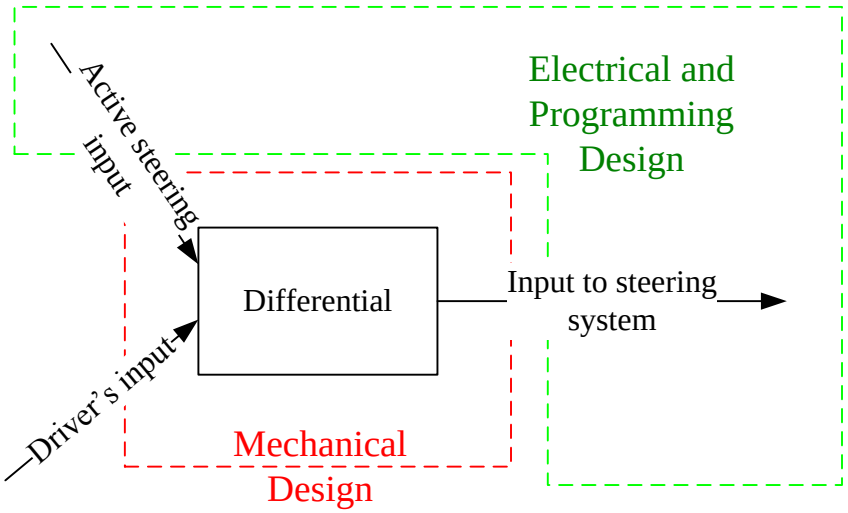

Figure 4.5: HIL experiment setup overview

The input coming from the active steering controller should be controllable through the pulse signal parameters. The previously proposed method of using a mechanism had difficulties in changing the pulse signal parameters. After considering other options it was found that the most convenient method was through the use of a control motor.

From all the above initial design considerations, as well as others not mentioned here, the differential option seemed to be the most viable to build the potential experiment around.

4.2 Overall Experiment Design

The differential will be used to combine two inputs: the driver's steering input and the controller's input, into one single output that will be fed into the steering system of the vehicle. The initial consideration was to mount the differential on a real vehicle for experimentation. However, this consideration was put aside for many difficulties. The other consideration was to use the differential setup to build a Hardware in the loop (HIL) simulation. A HIL simulation will enable the inclusion of real driver's interface during running a software vehicle simulation in real-time.

To enable a HIL simulation, interaction with a real-time software platform is required. Information, via sensors and signals, will be sent from the experiment setup to the real-time vehicle model program for computational analysis. Based on the analysis results, the active steering controller would intervene to change the steering command fed into the real-time program which will change the vehicle dynamics. Figure 4.5 shows an overview of the HIL experiment setup.

The overall setup design is divided into two main categories; the mechanical design and the electrical and programming design. Each category will be presented

Figure 4.6: Differential shaft locations and numbering

separately in the upcoming sections.

4.3 Mechanical Design

A differential has three shafts connected to it. Each shaft has a fixed ratio with each of the other two shafts when the third shaft is held fixed. The ratios are depicted in Table 4.1. Counterclockwise rotation when looking from the shaft's side is considered to be a positive rotation. The shafts are numbered in Figure 4.6.

Shaft Number	1	2	3
1	1:1	1:1.83	1:-1
2	1:0.545	1:1	1:-0.545
3	1:-1	1:-1.83	1:1

Table 4.1: Differential gear ratios for all combinations

The driver's steering wheel is recommended to be collinear with the output of the differential, as in normal passenger vehicles. Therefore the driver's input was chosen to come through shaft 1 and the output to come out of shaft 3. Shaft 2 was suitable to be used for the active steering controller input because the differential has a ratio of 1:-0.545 between shafts 2 and 3. This will increase the torque fed into the differential which in turn will lower the torque requirements from the control system's motor.

Amplitude of pulse (degrees measured at front tires)	**Frequency of pulse** (Hz)	**Maximum motor torque** ($T_{m_{max}}\ Nm$)
2°	1	3.37
	2	13.5
	3	30.4
	4	54.0
3°	1	5.06
	2	20.2
	3	45.5
	4	81

Table 4.2: Control motor's maximum required torque for different pulse parameters

Sizing the control system's motor was also a major mechanical design factor. There are many factors that contributed to sizing the control motor correctly. For example, the required speed from the motor increases with an increase in the amplitude and frequency of active steering pulse signal.

For this application, the specifications of the motor that are of most interest are the maximum torque and rated power. The maximum torque rather than the rated torque is required, due to that the motor will only run during the permissible controller's intervention which will be a relatively short period of time. During this short period, where the motor is used to input a pulse signal, the motor will operate on a wide range of speed and torque rather than at a constant value.

The maximum torque supplied by the active steering control system's motor should be more than the maximum torque required to input a certain pulse signal. The maximum torque required to input a certain pulse was calculated based upon the different components the torque will pass through to reach the vehicle's front tires. Simulation results presented in Section 3.5.2 show that it can be reasonably assumed that the whole steering system resistance to the steering wheel angular motion can be approximated to turning a mass moment of inertia equal to 0.05 kgm^2 (for a vehicle of the same parameters as of the Adams/Car vehicle model). Taking this into consideration, the maximum torque required from the control system's motor, $T_{m_{max}}$, can be evaluated as follows:

$$T_{m_{max}} = I_{sw}\alpha_{\delta_{mc}(t)}$$

where $\alpha_{\delta_{mc}(t)}$ is the control motor signal's angular acceleration. The ratio between the control motor's signal and the tire's control steering angle consists of the dif-

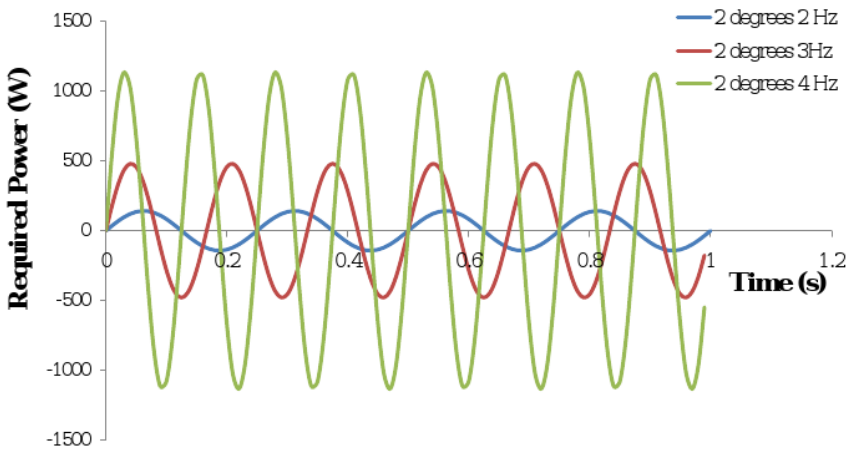

Figure 4.7: Required power for different pulse parameters

ferential's ratio between shafts 2 and 3 multiplied by the vehicle's steering ratio.

$$\alpha_{\delta_{mc}(t)} = S_{R_d(2:3)} S_R \alpha_{\delta_c(t)}$$

$\alpha_{\delta_c(t)}$ will greatly depend upon the pulse signal parameters. A study was done to assess the motor's maximum required torque, $T_{m_{max}}$, with respect to the different parameters of the pulse signal. Table 4.2 shows $T_{m_{max}}$ with respect to frequency and amplitude of a symmetric pulse.

The equation: $T_{sw}\omega_{sw}$, was used to evaluate the required power to produce the control's pulse signal. This was useful in determining the motor's required rated power. Figure 4.7 shows a plot of the required torque for different pulse parameters. The figure shows that by increasing the frequency a higher power rated motor will be required. It also shows that to produce a 4 Hz symmetric pulse it will require about a 1 kW control motor, which is relatively big to be used in this steering system.

From the values presented in this section, in Table 4.2 and Figure 4.7, it was decided that a motor having a rated power of around 600 W and a maximum torque of 30 Nm would be suitable. By doing so, a pulse of the same amplitude of 2° (at the tire's level) for any frequency up to 3 Hz can be achieved. The motor plus gear box actually used had a rated power of 660 W and a peak torque of 32 Nm. The complete specifications of the motor are shown in Appendix B.3.

One problem that required a solution was that the differential used is what is known as an open differential. An open differential simply allows motion to the port having less resistance. Having no device to constrain motion throughout the differential would cause problems in using the differential appropriately. A mechanical brake was considered to be mounted on port 2 so that during the time the control motor is not active the brake is on and therefore port 2 is held fixed. This will allow the use of the differential in a way that is suitable for this experiment. A CAD model of the differential with all its attachments is shown in Figure 4.8.

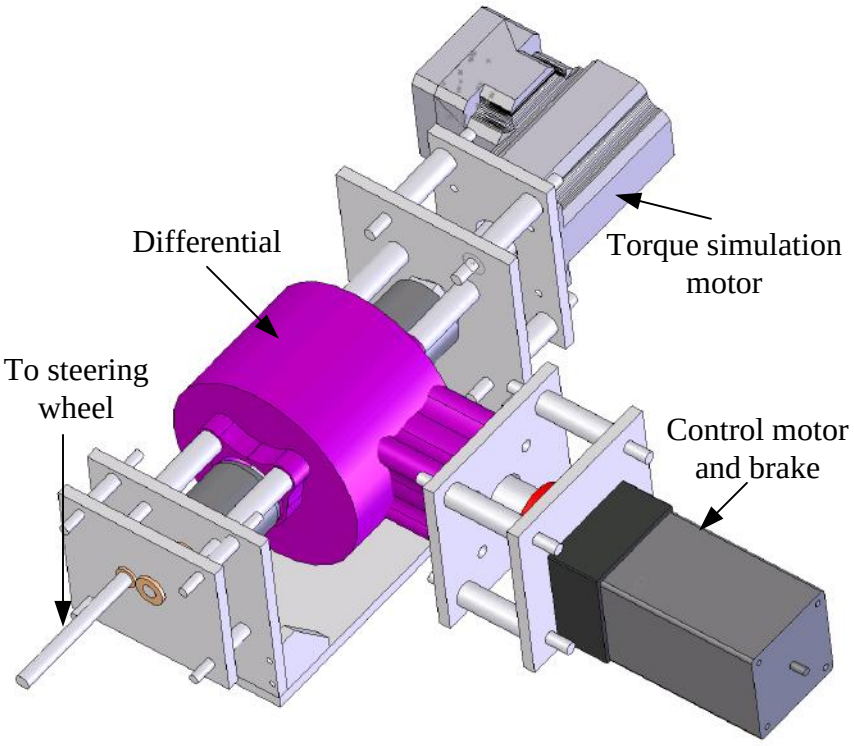

Figure 4.8: CAD model of the differential with its attached components

The differential with all its attached components was required to be mounted on a surface for the experiment. The initial consideration was to simply mount the differential on a steel table to lower vibrations and to compensate for the torques in the differential during experimentation. However, it was decided to build a custom stand for the differential. This was preferable for many reasons. Firstly, having a custom stand for the differential will make the whole experiment setup one piece that will not require any dissembling if for instance its location was required to change. Secondly, a driver's seat can be designed to be part of the stand such that the weight of the driver can compensate the torque coming from the differential during experimentation. Thirdly, the stand can be designed such that the differential will be mounted at an angle close to passenger vehicle steering wheel's tilt angles. This will give the driver a more ergonomic feel and grip of the steering wheel. The angle used, which is in the range of passenger vehicle's steering wheel tilt angles, was 20°. Figure 4.9 shows a 3D CAD model of the stand design prior to building it.

4.4 Electrical and Programming Design

This section will focus on various issues in the electrical and programming design of the experiment that were considerably more important as compared with the

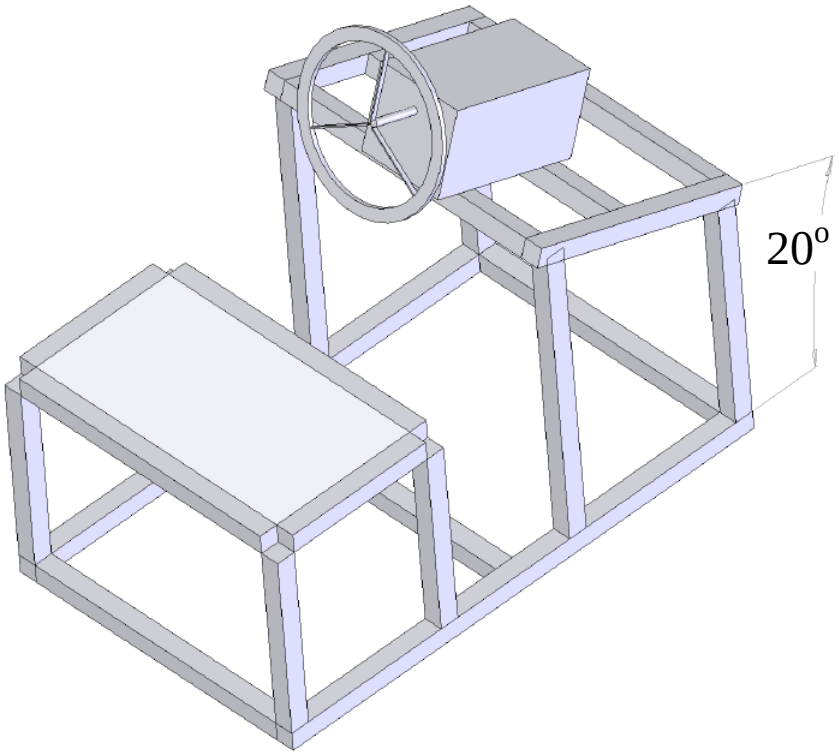

Figure 4.9: Experiment stand design

remaining design aspects. Design aspects related to electrical and hardware design will be presented first, followed by the programming design of the experiment.

4.4.1 Electrical Design

As mentioned before, the initial idea was to mount the final setup onto a vehicle, but due to difficulties this was disregarded. The other idea which was eventually implemented was to use a motor to simulate the steering column torque based upon the calculated vehicle dynamics. This motor would be mounted on port 3 of the differential as shown in Figure 4.6. The constraints on choosing the torque motor were few, the main constraint was that the simulation motor should be capable of supplying the resistive torque required. The resistive torque to the steering wheel was approximated, with a good degree of accuracy, by rotating a 0.05 kgm^2 mass moment of inertia body, as mentioned previously. From the ratios shown in Table 4.1, the simulation motor would require around twice the maximum torque of what the control motor has. But due to this being the only major constraint, it was easily satisfied by placing a gear head, to increase the torque, on the simulation motor. A gear head having a ratio of 12:1 and a motor able to supply a maximum torque of around 8 Nm were used for the simulation motor. This would give a maximum torque of 96 Nm, which was enough to cover the requirements.

Another major design aspect was choosing between an analog or digital controller plus amplifier combination. The differences between analog and digital systems are quite complex and choosing between the two systems is not intuitive. But due to available hardware, it was decided to choose an analog controller and amplifier combination for both the control motor and simulation motor.

Feedback is an important feature to improve control systems. The motor as well as the driver's inputs to the experiment need to be monitored to firstly provide inputs to the vehicle model in the simulation program, and secondly to provide a feedback signal to lower deviations from the desired system's output. The kind and amount of feedback devices as well as their location in the experiment setup were required to be determined. Although the differential shown in Figure 4.6 has three ports, and the inputs and outputs of each port are required to be monitored for the experiment to work successfully, two feedback devices mounted on two of the three ports were enough for achieving the requirements. By using Table 4.1, knowing the displacement of two ports would allow knowing the third port's displacement. Due to other factors, such as mounting space and cost of feedback devices, the two ports that had a feedback mounted onto them were ports 2 and 3 of the differential. The driver's input, which is at port 1 of the differential could be evaluated by: $\theta_1 = \theta_3 - 1.83\theta_2$, where θ corresponds to angular displacement with respect to each of the subscripted port numbers.

The controller used is a Data-Acquisition-Card board that contains analog and digital inputs and outputs as well as encoder feedback 5 and 10 pin plugs. The Data-Acquisition-Card allows for interfacing with Matlab/Simulink. The DAQ board was used to gather inputs through the feedback devices and depending upon the computational analysis done in Matlab/Simulink would send out signals to the appropriate hardware. Figure 4.10 presents the overall setup of the electrical hardware and their respective connections whereas Figure 4.11 shows the experimental setup after assembling. A list of all the components used in the experiment setup with their respective product numbers and manufacturers is shown in Appendix B.1.

4.4.2 Programming Design

The DAQ board used allowed for all the control programming to be done in Matlab/Simulink. The vehicle model used in this experiment was the same as the DynaFlexPro vehicle model introduced earlier in section 3.3. Unlike the simulations done in Chapter 3, this HIL simulation required a controller to determine when the control motor should intervene with the pulse signal. As a start for the experiment it was decided to fix the pulse parameters from changing during the simulation runs. Meaning that the controller will not determine which parameters to intervene with but instead would only determine when to intervene with the predefined pulse parameters. Having the controller to determine the pulse parameters would give better results, but this experiment project was to prove the concept of pulse active steering rather than optimizing the pulsed active steering system.

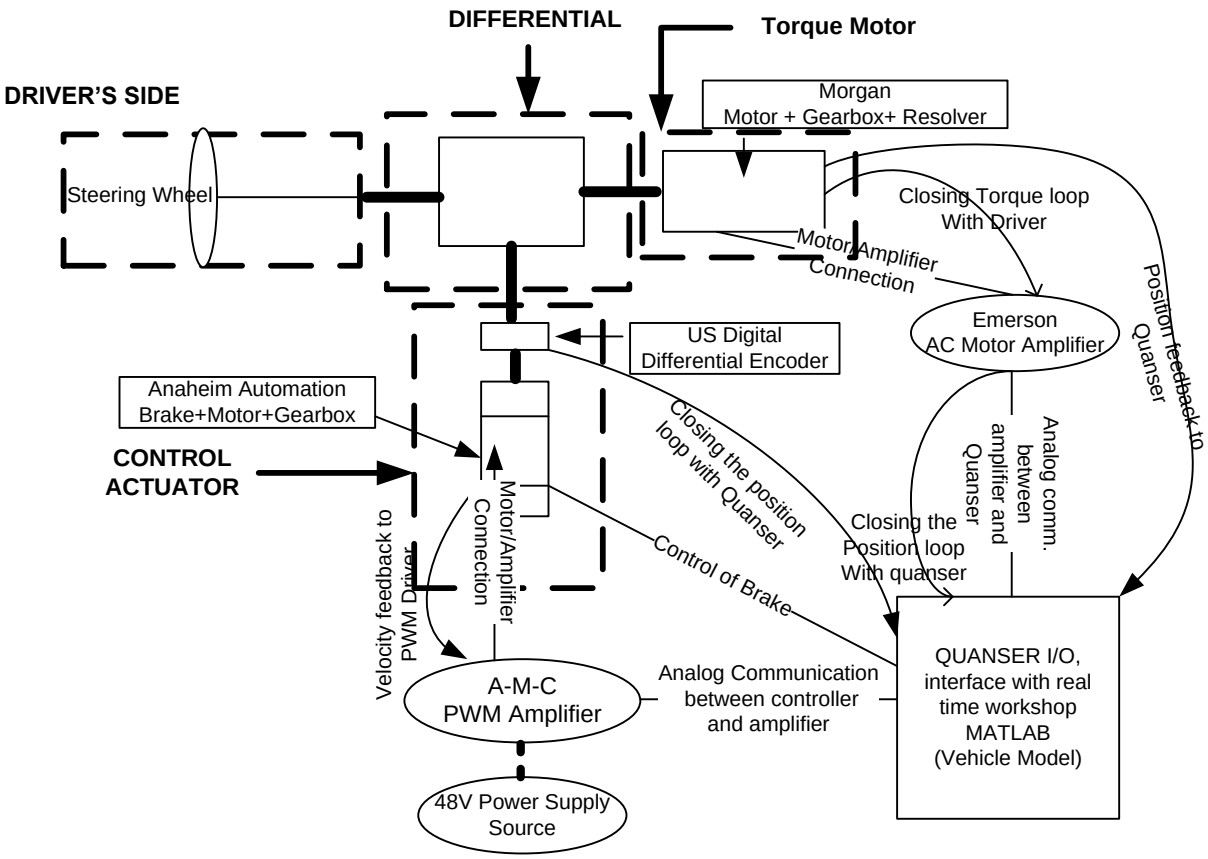

Figure 4.10: Experiment overview of electrical setup

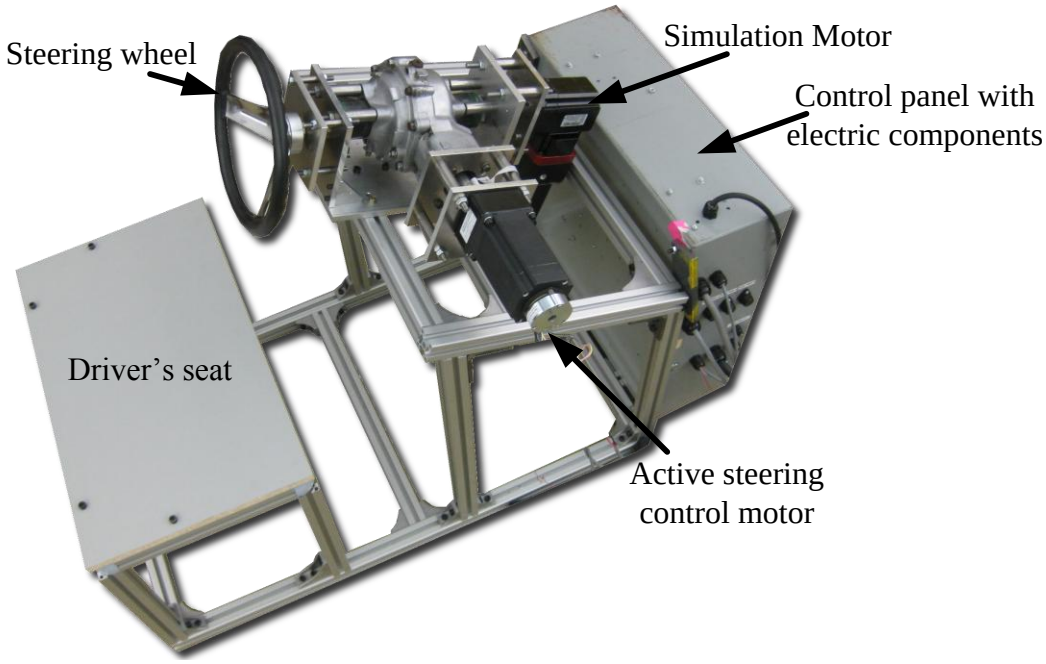

Figure 4.11: Experiment setup after assembling

The program firstly calculates the driver's steering input based on the encoders' readings from ports 2 and 3 of the differential. The driver's steering input is fed into the vehicle model to calculate the present vehicle states. These vehicle states are used to calculate the rollover coefficient R as well as the actual and desired yaw rates. The controller will check whether R surpasses a threshold, and also will calculate the actual to desired yaw rate deviation. Preference is given to the former over the latter. A threshold of 0.8 (positive or negative) for R was chosen to allow for the system time lag before R reaches the limit of 1 or -1. If R surpasses the threshold, the controller would signal for the control motor to intervene to subtract a pulse signal with predefined pulse parameters. If R is in the range of [-0.8,0.8], then the controller will check the yaw rate deviation, if it exceeds a certain amount then the controller would command the control motor to add the pulse signal with the predefined pulse parameters. It was also required to make sure that the control motor would not stop before completing an addition or subtraction of a full pulse cycle. Not doing so will cause an offset to the driver's steering control of the vehicle model. The control program as well would turn the brake off during the control motor's intervention. A simple control algorithm is shown in Figure 4.12.

4.5 Experimental Results

Many problems arouse while assembling the various experiment components together. Troubleshooting was a major stage in putting the experimental setup to work. Eventually, through the help of the technical support centers of the companies for different components used, the setup was successfully working. Two sets of experiments were implemented. The first set consisted of running the setup with a steering input similar to the driver's steering input used in the DynaFlexPro vehicle model simulations of this project, i.e. a J-turn maneuver. The objective of the first set was to compare the simulation results with experimental results. The second set consisted of letting a human driver interact with the experiment setup. The objective was to assess whether the active steering control system will be able to prevent a human driver from rolling over the vehicle model through anonymous steering inputs. Each set of experiments will be presented separately in the following sections.

4.5.1 Validating Simulation Results

In this experiment set, the steering wheel was held fixed and the experiment program was modified such that the steering input was similar to that used in section 3.3 for the driver's input. The driver's steering input used here was larger in magnitude compared to that used in section 3.3. This was required because the results depicted in section 3.3 show that the resulting rollover coefficient approaches 1 only at the beginning of the simulation. If the same driver's input was used in the experiment the controller would only intervene at the beginning of the experiment,

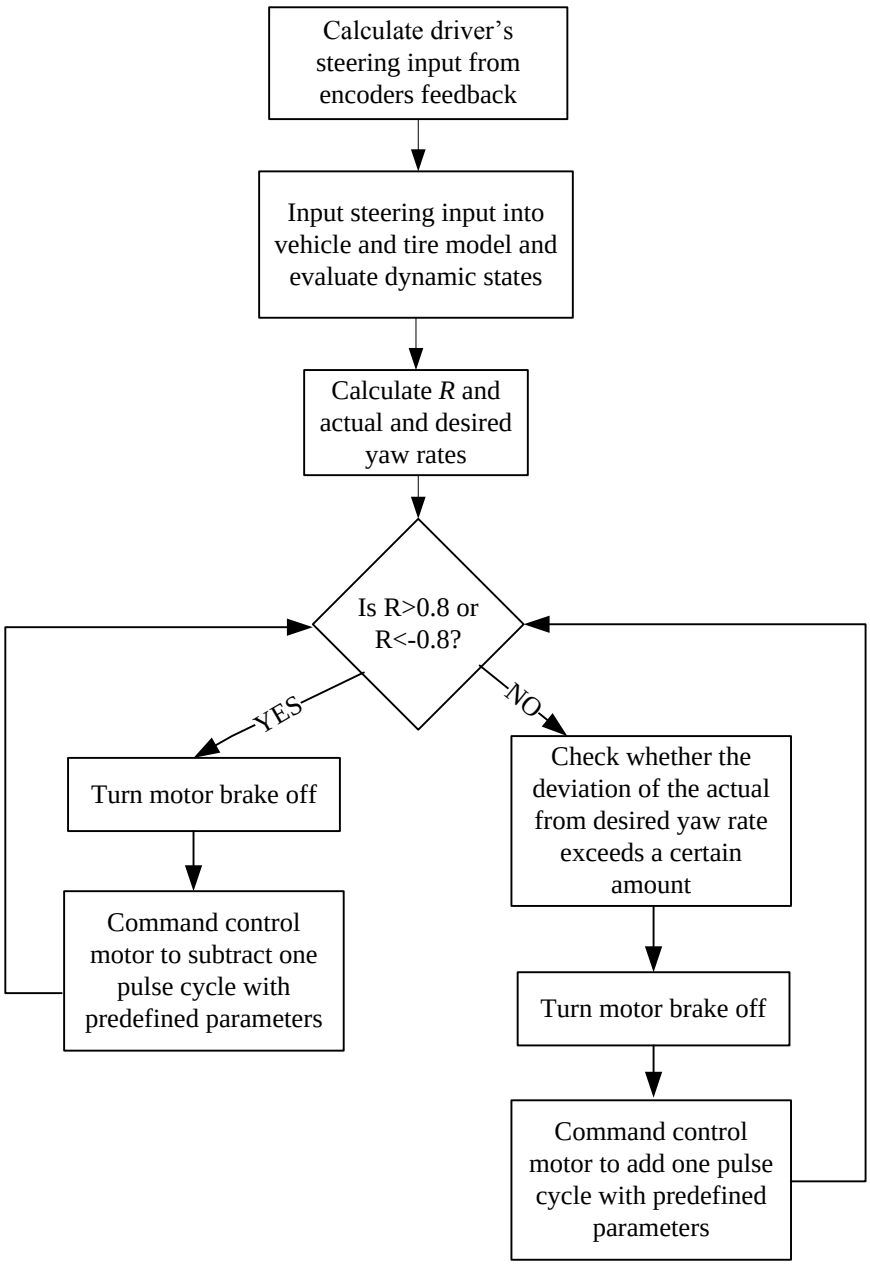

Figure 4.12: Control algorithm of experiment

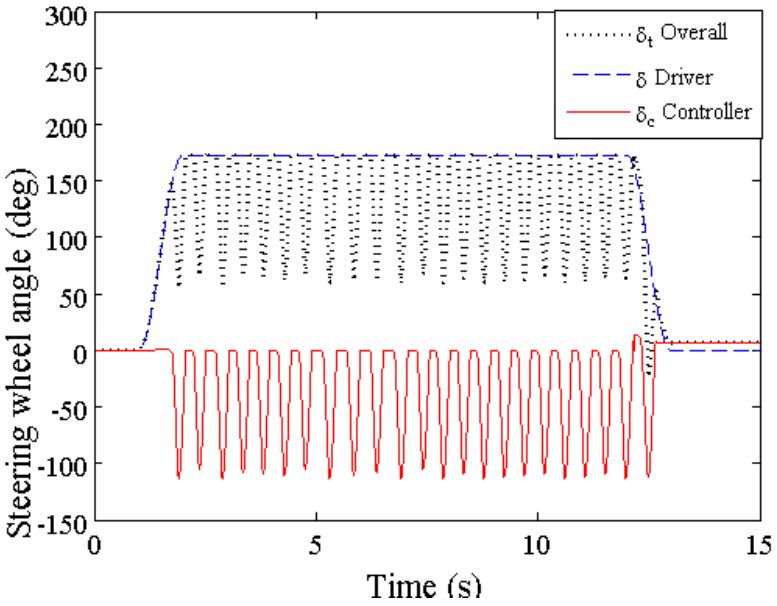

Figure 4.13: Steering inputs for first simulation run

where R is approaching a value of 1. By increasing the magnitude of the steering input, the rollover coefficient will increase and therefore the controller would intervene more regularly. This will help better in evaluating the controller and the system as a whole.

In the first experiment run the active steering controller's symmetric pulse was predefined to have a frequency of 3 Hz, an amplitude of 3° as measured from the tires. Figure 4.13 shows the steering inputs of the driver, the controller, as well as the overall steering command, whereas Figure 4.14 shows a plot of the rollover coefficient throughout the simulation run.

Figure 4.13 shows that the active steering controller intervened very soon after the start of the simulation. That was due to the rollover coefficient surpassing the threshold value of 0.8 as shown in Figure 4.14. The intervention was continuous to nearly the end of the simulation because the rollover coefficient during that period was surpassing the threshold value that commands the controller to intervene. However, Figure 4.14 shows that R did exceed the limit of 1 at various instances which shows that the pulse parameters used for this simulation run were not appropriate to strictly keep R in the allowed range.

Based upon the first simulation run, it was decided that a second simulation run should be done using the same pulse parameters but changing the pulse amplitude from 3° to 4°. A plot of the second simulation run's steering inputs is shown in Figure 4.15, whereas Figure 4.16 shows a plot of the rollover coefficient throughout the simulation run.

Figure 4.15 shows that the controller intervened close to the start of the simulation run. This was due to R approaching the limit of 1 at the same interval of the

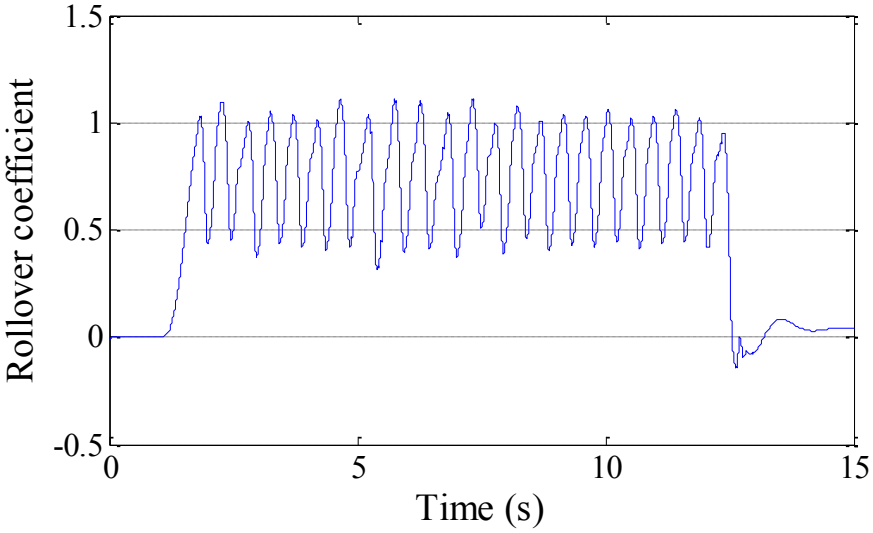

Figure 4.14: Rollover coefficient throughout first simulation run

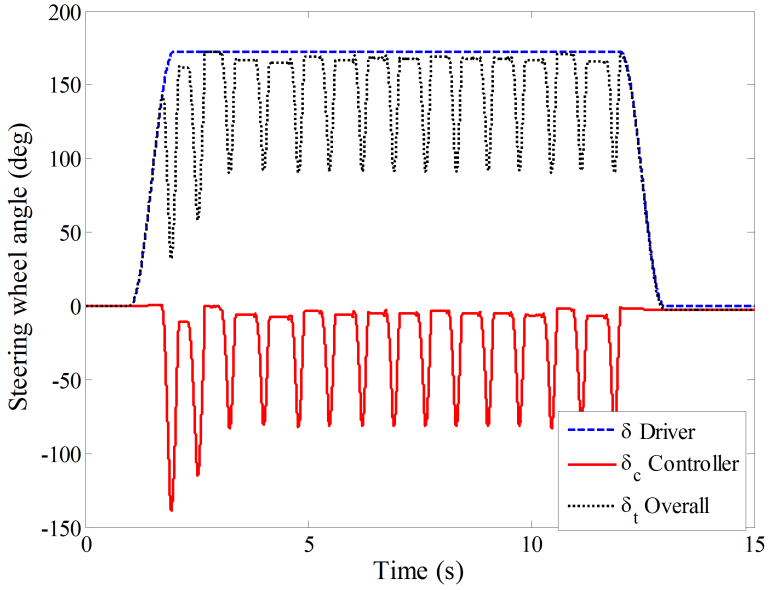

Figure 4.15: Steering inputs for second simulation run

controller's intervention, as shown in Figure 4.16. This simulation run shows that changing the amplitude had a major effect in lowering R to under the upper limit throughout the whole simulation time. As well, the number of complete pulse cycle interventions the 4° pulse did were much lower than that of the 3° pulse simulation run.

The experiment results shown in this section strongly support the simulation results shown in section 3.3. The experiment results showed that by intervening

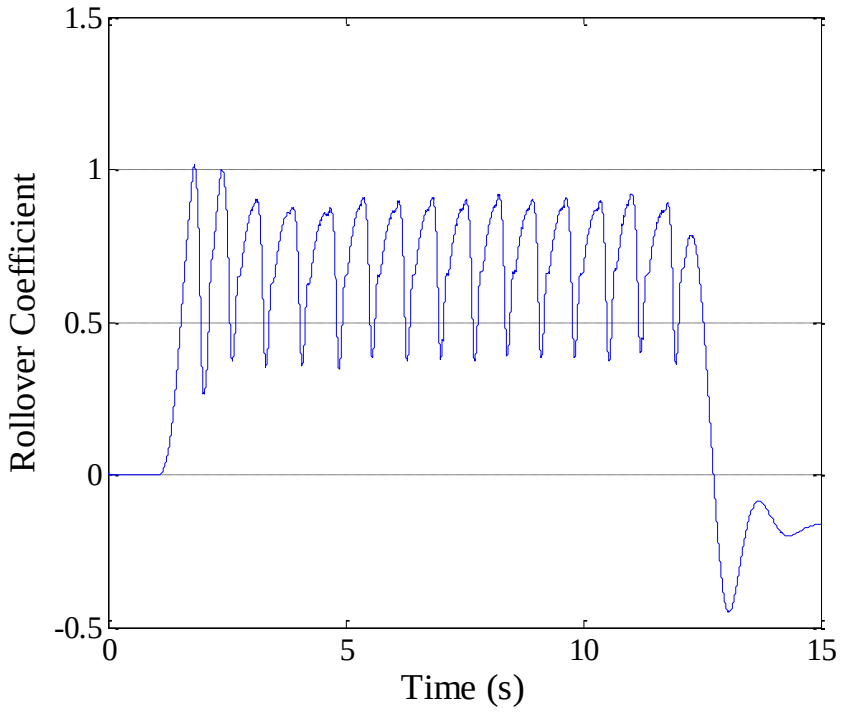

Figure 4.16: Rollover coefficient throughout second simulation run

with the controller's pulse signal the rollover coefficient can be lowered. The results show as well that the amplitude of the controller's pulse has a significant effect on the rollover coefficient and by increasing the amplitude the rollover coefficient can be lowered significantly.

4.5.2 Anonymous Driver Input

In this simulation set, a human driver was asked to input a random steering input such that he tries to roll over the vehicle in a period of 15 seconds. The control motor signal's parameters were predefined prior to the simulation run, this will cause the controller to only evaluate when to intervene with the pulse and not to evaluate the selection of the pulse parameters. The first run consisted of setting the pulse parameters to a symmetric pulse with an amplitude of 3° at the tires level and a frequency 2 Hz. Figure 4.17 shows the plots of the driver's steering input, the controller's intervention and the overall steering input to the vehicle model. Figure 4.18 shows a plot of the rollover coefficient throughout the simulation run.

Figures 4.17 and 4.18 show that the controller was successful to intervene at 5 separate periods in which the rollover coefficient was close to crossing a value of 1. The intervention of the controller in all periods was only a 1 pulse cycle, this was because the value of R after the completion of 1 cycle became lower than the threshold value of 0.8. However, close to the 6 second mark on Figure 4.18 the rollover coefficient slightly surpasses the value of 1. This could mean that the

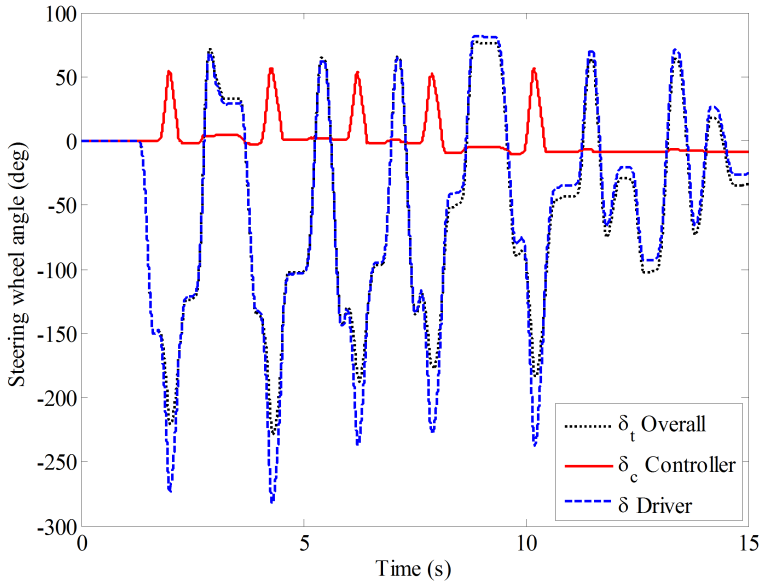

Figure 4.17: Steering inputs for first simulation run

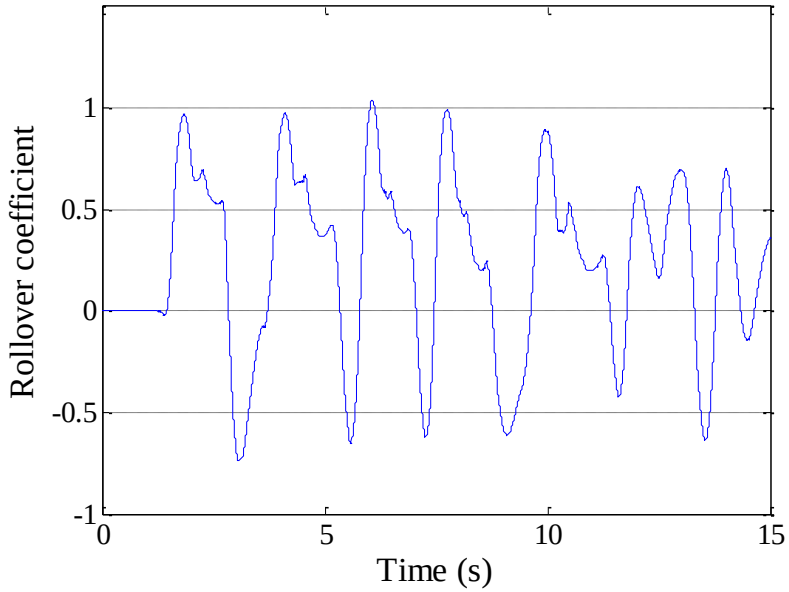

Figure 4.18: Rollover coefficient throughout first simulation run

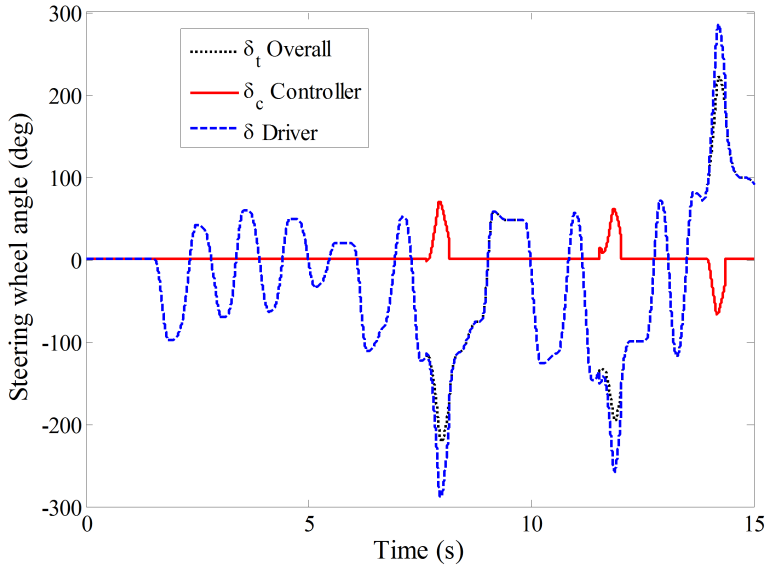

Figure 4.19: Steering inputs for second simulation run

vehicle would have rolled over at this instant and leads to the conclusion that the amplitude of the pulse signal required to be higher to prevent this from occurring.

In the second simulation run the amplitude of the pulse signal was increased from 3° to 4° to see whether that would be enough to prevent R from surpassing the limits of 1 or -1. Figures 4.19 and 4.20 show that the controller intervened 3 times, twice in one direction and the last intervention in the other direction. In this run, the rollover coefficient was successfully kept between the limits of 1 and -1. This shows the importance of having amplitude modulation during the controller's intervention to completely prevent the rollover coefficient from exceeding the limits.

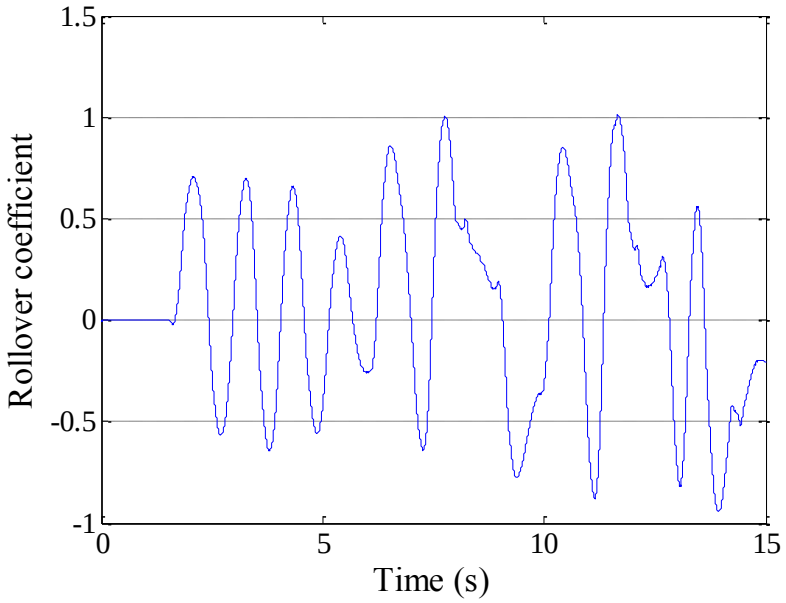

Figure 4.20: Rollover coefficient throughout second simulation run

Chapter 5

Conclusions and Future Work

5.1 Conclusions

This thesis was targeted on assessing various aspects of the newly introduced pulsed active steering system. It was divided into two main parts: a simulation part where different vehicle models were used in different simulation software, and an experimental part where a test bed experiment setup was designed and assembled to run hardware-in-the-loop simulations.

The simulation part was divided into three categories. The first category consisted of using an analytical hand-derived model to assess the effect of the active steering system pulse's frequency modulation on the vehicle's yaw and roll dynamic response. Results show that frequency modulation has no effect on the yaw dynamics, in addition the roll dynamics were improved by an increase in pulse's frequency. However, the improvement in the roll dynamics becomes more minor at higher frequencies. This led to the conclusion that frequency modulation could improve the roll dynamics of the vehicle only to a certain limit. This means that if the active steering pulse signal was only controlled through its frequency, rollover still might occur in driving maneuvers beyond the capacity of frequency modulation.

The conclusion of the first category under the simulation part of this research project led to the second category. The second category consisted of assessing the effect each of the pulse's parameters has on the yaw and roll dynamics of the vehicle model. The pulse parameters assessed were the amplitude, frequency and pulse pattern. To gain more reliable results as compared with the first category's hand-derived model, a more complex vehicle model built using DynaFlexPro simulation software was used for the second category simulation runs.

Results obtained in the second category were more informative. The amplitude of the pulse would improve the roll dynamics of the vehicle in compromise of the yaw dynamics. Meaning that to prevent a rollover from taking place by increasing the amplitude of the pulse active steering system, the vehicle is forced to deviate from its desired path. This is common, even among conventional active steering

systems, where there is a compromise between roll and yaw dynamics. Since roll stability is given a priority over yaw stability, pulse amplitude modulation would be beneficial at such instances.

As for the pulse frequency modulation, the DynaFlexPro model simulations showed interesting results. Results show that different pulse frequencies, with the same amplitude, have similar effect on the yaw dynamics. Therefore, frequency modulation does not improve the yaw dynamics. However, frequency modulation has an effect on the roll dynamics of the vehicle when the active steering pulse is subtracted from the driver's command. Results show that having the pulse frequency set equal to the vehicle's first roll natural frequency improves the roll dynamics the most. This conclusion was unexpected since usually systems are designed to operate far from their natural frequencies. However, by subtracting the active steering pulse, the vehicle is forced to vibrate at resonance in the opposite direction away from rolling over. This conclusion was not analogous to that observed in the first category and this was because a more complex model was used in the second category and thus being more reliable.

Pulse pattern modulation did show that it has an effect on both: the yaw dynamics as well as the roll dynamics. However, no solid conclusion could be extracted from the results. It was recommended that a separate study to assess the optimal pulse pattern should be done.

The third category under the simulation part of this project was to gain numeric values to help in sizing various components in the experimental setup. A valuable result of this category worth of mentioning here was that the resistance felt at the steering wheel due to the different component of the steering system in the Adams/Car model used could be approximated, to a good degree of accuracy, to turning a body having a mass moment inertia of 0.05 $kg.m^2$. This was directly used in the calculations for sizing the control system motor.

The second part of this research project was building and implementing an experiment. A test bed was put together to be used for current and future research experiments related to active steering. The experiments done on the test bed in this research project was firstly to validate the results obtained in the simulations part of the project. Secondly to assess the applicability of pulse active steering and whether the active steering controller will be able to prevent rollover from taking place. The experiment runs performed on the test bed show that their respective results are similar to the simulation results. As well, experiment runs were performed to assess whether the active steering system was capable of preventing a human driver from rolling over the vehicle model, which the controller did successfully.

The results obtained from both parts of this research project show that pulse active steering has good potential to improve the performance of active steering systems. This research project provides the necessary information to build a robust controller for a pulse active steering system. A proposed controller structure, based upon this research project, is to have the amplitude of the pulse signal to act as the proportional gain of the feedback controller. The frequency will be fixed at the roll

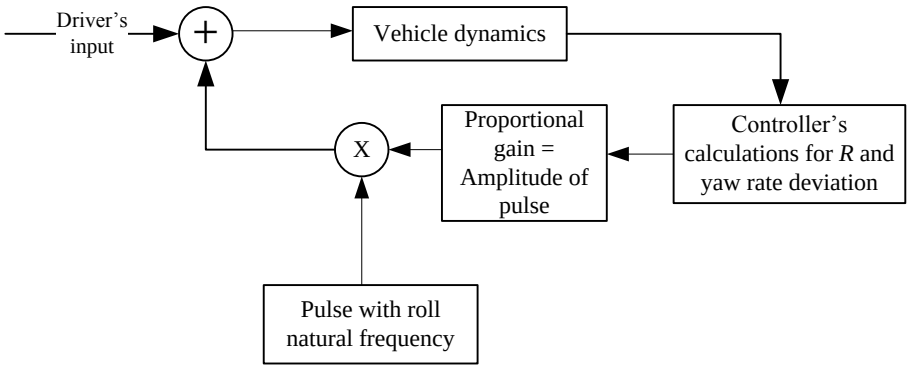

Figure 5.1: Proposed controller structure

natural frequency of the vehicle. The optimal pulse pattern though still needs to be researched. Figure 5.1 shows a block diagram of the proposed control structure.

5.2 Future Work

This research project has opened several doors for future work consideration. It also included building a test bed that could be used as a platform for future active steering research related projects.

As mentioned previously in this thesis, the effect of the pulse pattern parameter on the vehicle dynamics required additional research. A proposed future work to this research project is to conduct a study on optimizing the pulse pattern for optimal vehicle dynamics. By doing so, all pulse parameters are assessed and an optimal controller can be designed.

Another possible future work is concerning the proposed controller structure, presented in the conclusions section of this thesis. The proposed controller needs to be designed and evaluated through experiments using the test bed setup. It is expected that the proposed controller, that allows for the pulse amplitude to be modified during simulation runs, will give even better results than predefining the pulse parameters.

Another future work to be considered, which is highly recommended, is to study the integration of pulsed active steering alongside other active safety vehicle systems such as the ESC. Research has shown that active safety systems working together provide more stability and safer vehicles. It will be interesting to compare present active safety system integrations with and without including pulsed active steering.

Finally, this work will eventually require to be assessed through a real vehicle experiment setup. This will ensure that all factors of real driving, whether from the vehicle or from the driver, are taken into consideration.

References

[1] Adams/car website. `http://www.mscsoftware.com/products/products_detail`, Accessed July 2009. 11

[2] Leading causes of death. `http://www.cdc.gov/nchs/FASTATS/lcod.htm`, Accessed July 2009. 1

[3] M. Abe and Y. Furuawa. A direct yaw moment control for vehicle yaw rate model following control-comparison with 4ws. Nwagboso, 1997. 5

[4] J. Ackermann. Verfahren zum lenken von strabenfahrzeugen mit vorder und hinter- radlenkung, 1993. 7

[5] J. Ackermann. Advantages for active steering for vehicle dynamics control. Vienna, 1999. Proc. International Symposium on Automotive Technology and Automation. 5, 8

[6] J. Ackermann and T. Bunte. Yaw disturbance attenuation by robust decoupling of car steering. *Control Engineering Practice*, 5(8):1131–1136, 1997. 8

[7] J. Ackermann, T. Bunte, W. Sienel, H. Jeebe, and K. Naab. Driving safety by robust steering control. In *Int. Symposium on Advanced Vehicle Control*, 1996. 8

[8] J. Ackermann and D. Odenthal. Damping of vehicle roll dynamics by gain scheduled active steering. In *European Control Conference*, 1999. 22

[9] R. W. Allen, H. T. Szostak, D. H. Klyde, T. J. Rosenthal, and K. J. Owens. Vehicle dynamic stability and rollover. *NASA STI/Recon Technical Report N*, 93:30828–+, June 1992.

[10] G. Box and N. Draper. *Empirical Model-Building and Response Surfaces*. Wiley, 1987. 13

[11] J. Fenton. *Handbook of Automotive Design Analysis*. Mercury House Business Publications Ltd., 1973. x, 37

[12] T. Fukao, S. Miyasaka, K. Mori, N. Adachi, and K. Osuka. Active steering systems based on model reference adaptive nonlinear control. In *IEEE Intelligent Transportation Systems Proceedings*, pages 502–507, 2001. 6

[13] Y. Hirano and K. Fukatani. Development of robust active rear steering control for automobile. *Transactions of the Japan Society of Mechanical Engineers, Part C*, 62:1753–1758, 1996. 6

[14] S. Horiuchi, K. Okada, and S. Nohtomi. Effects of integrated control of active four wheel steering and individual wheel torque on vehicle handling and stability - a comparison of alternative control strategies. *Vehicle System Dynamics*, 33:680–691, 2000. 4

[15] J. Kasselmann and T. Keranen. Adaptive steering. *Bendix Technical Journal*, 2:26–35, 1969. 5, 7

[16] J. Kerr. Auto tech: Bmws active steering. Canadian Driver. `http://www.canadiandriver.com/2003/11/12/auto-tech-bmws-active-steering.htm`, Accessed July 2009. 2

[17] W. Kramer and M. Hackl. Potential functions and benefits of electronic steering assistance. In *XXXVI Fisita Congrass*, June 1996. 7

[18] C. C. Kuo. Sports utility vehicle rollover control with pulsed active steering control strategy. Master's thesis, University of Waterloo, 2005. 7, 10

[19] S. Lee, U. Lee, S. Ha, and C. Han. Four-wheel independent steering (4wis) system for vehicle handling improvement by active rear toe control. In *JSME Int.J.Ser.C*, volume 42, pages 947–956, 1999. 6

[20] S. Mammar and V. B. Baghdassarian. Two-degree-of-freedom formulation of vehicle handling improvementby active steering. volume 1 of *6*, Chicago, IL, 2000. American Control Conference, 2000. Proceedings of the 2000. 4, 6

[21] K. Morency. Automatic generation of real-time simulation code for vehicle dynamics using linear graph theory and symbolic computing. Master's thesis, University of Waterloo, 2007. 24

[22] S. Mykherjee. Rollover crash analysis of the rtv using madymo. In *SAE Symposium of International Automotive Technology*, number 05-0186. Indian Institute of Technology Delhi, 2005. 26

[23] M. Nagai, M. Shino, and F. Gao. Study of integrated control of active front steer angle and direct yaw moment. *SAE Journal*, 2001. 6

[24] E. Ono, S. Hosoe, H. D. Tuan, and S. Doi. Robust stabilization of vehicle dynamics by active front wheel steering control. In *Proceedings of the 1996 35th IEEE Conference on Decision and Control*, pages 1777–1782, 1996. 6

[25] H. Pacejka. *Tire and Vehicle Dynamics*. SAE International, 2005. 16, 18

[26] R. Rajamani. *Vehicle Dynamics and Control*. Springer, 2006. 15

[27] W. Sienel. Estimation of the tire cornering stiffness and its application to active car steering. In *Proceedings of the 1997 36th IEEE Conference on Decision and Control. Part 5 (of 5)*, pages 4744–4749, 1997. 6

[28] D. O. Tilman, T. Bnte, and J. Ackermann. Nonlinear steering and braking control for vehicle rollover avoidance. In *European Control Conference*, 1999. 8, 9

[29] Maplesoft website. Looking for dynaflexpro? `http://www.maplesoft.com/products/thirdparty/dynaflexpro/`, Accessed July 2009. 11

[30] Mathworks website. Product list. `http://www.mathworks.com/products/`, Accessed July 2009. 12

APPENDICES

Appendix A

Vehicle Model Parameters and Initial Conditions

A.1 DynaFlexPro

Body	Mass (kg)	Rotational Inertia ($kg.m^2$)					
		I_{xx}	I_{yy}	I_{zz}	I_{xy}	I_{xz}	I_{yz}
Vehicle Body	2077	330	1925	1925	0	110	0
Lumped mass	10	1.0	0.5	1.0	0	0	0
Tires	28	0.78	1.56	0.78	0	0	0

Table A.1: Inertia properties of vehicle model

Spring/Damper	Stiffness (N/m)	Free Length (m)	Damping (Ns/m)
Front Corner (R/L)	48289	0.674	3075
Rear Corner (R/L)	30518	0.72	2331
Tires (all corners)	3.04×10^5	0.355	500

Table A.2: Spring/damper properties of vehicle model

State Variable	Initial Value	Description
$v_x(t)$	20	Velocity of COM_1 along x_1 (m/s)
$v_y(t)$	0	Velocity of COM_1 along y_1 (m/s)
$v_z(t)$	0	Velocity of COM_1 along z_1 (m/s)
$\frac{d}{dt}s_1(t)$	0	Rate of front left suspension extension along z_1 (m)
$\frac{d}{dt}s_2(t)$	0	Rate of front right suspension extension along z_1 (m)
$\frac{d}{dt}s_3(t)$	0	Rate of rear left suspension extension along z_1 (m)
$\frac{d}{dt}s_4(t)$	0	Rate of rear right suspension extension along z_1 (m)
$\frac{d}{dt}yaw(t)$	0	Yaw rate of COM_1 about z_1 (rad/s)
$\frac{d}{dt}pitch(t)$	0	Pitch rate of COM_1 about y_1 (rad/s)
$\frac{d}{dt}roll(t)$	0	Roll rate of COM_1 about x_1 (rad/s)
$\frac{d}{dt}\phi_1(t)$	57.45	Spin rate of front left tire (rad/s)
$\frac{d}{dt}\phi_2(t)$	57.45	Spin rate of front right tire (rad/s)
$\frac{d}{dt}\phi_3(t)$	57.45	Spin rate of rear left tire (rad/s)
$\frac{d}{dt}\phi_4(t)$	57.45	Spin rate of rear right tire (rad/s)
tanslipangleTire1	0	Slip angle of front left tire (rad)
longslipangleTire1	0	Slip ratio of front left tire
tanslipangleTire2	0	Slip angle of front right tire (rad)
longslipangleTire2	0	Slip ratio of front right tire
tanslipangleTire3	0	Slip angle of rear left tire (rad)
longslipangleTire3	0	Slip ratio of rear left tire
tanslipangleTire4	0	Slip angle of rear right tire (rad)
longslipangleTire4	0	Slip ratio of rear right tire
$x(t)$	0	Position of COM_1 along x (m)
$y(t)$	0	Position of COM_1 along y (m)
$z(t)$	0.8995	Position of COM_1 along z (m)
$s_1(t)$	0.5632	Position of front left lump mass from ground along $z(m)$
$s_2(t)$	0.5632	Position of front right lump mass from ground along $z(m)$
$s_3(t)$	0.5617	Position of rear left lump mass from ground along $z(m)$
$s_4(t)$	0.5617	Position of rear right lump mass from ground along $z(m)$
$yaw(t)$	0	First 321 Euler Angle of (x_1, y_1, z_1) frame (rad)
$pitch(t)$	0	Second 321 Euler Angle of (x_1, y_1, z_1) frame (rad)
$roll(t)$	0	Third 321 Euler Angle of (x_1, y_1, z_1) frame (rad)
$\phi_1(t)$	0	Rotation angle of front left tire (rad)
$\phi_2(t)$	0	Rotation angle of front right tire (rad)
$\phi_3(t)$	0	Rotation angle of rear left tire (rad)
$\phi_4(t)$	0	Rotation angle of rear right tire (rad)

Table A.3: DynaFlexPro model's states with their respective initial values

A.2 Adams/Car Model

Definition	Unit	Value
Total vehicle mass	kg	1530
Vehicle sprung mass	kg	1430
Wheel base	m	2.56
Track width (front)	m	1.52
Track width (rear)	m	1.59
Distance from center of gravity to front axle	m	1.48
Distance from center of gravity to rear axle	m	1.077
Height of center of gravity above ground	m	0.432
Spring stiffness	N/m	1.25e5
Vehicle moment of inertia w.r.t. x-axis	$kg.m^2$	584
Vehicle moment of inertia w.r.t. y-axis	$kg.m^2$	6129
Vehicle moment of inertia w.r.t. z-axis	$kg.m^2$	6022

Table A.4: Parameters of Adams/Car vehicle model

Appendix B

Experiment

B.1 Experiment Setup Components

Manufacturer	Kollmorgen
Product Number	6SM47L-3000

Table B.1: Torque Motor

Manufacturer	Anaheim Automation
Product Number	BLY344D-48V-3200

Table B.2: Control Motor

Manufacturer	US Digital
Product Number	HB6M-2500-750-N-D-H

Table B.3: Optical Encoder

Manufacturer	Emerson
Product Number	LX-400

Table B.4: Torque Motor Amplifier

Manufacturer	Advanced Motions Control
Product Number	BX30A8

Table B.5: Control Motor Amplifier

Manufacturer	Mean Well
Product Number	SE-1000-48

Table B.6: Control Motor Power Supply

Manufacturer	Quanser
Product Number	MultiQ-3

Table B.7: DAQ Board

B.2 Gearbox Initial Design Algorithm

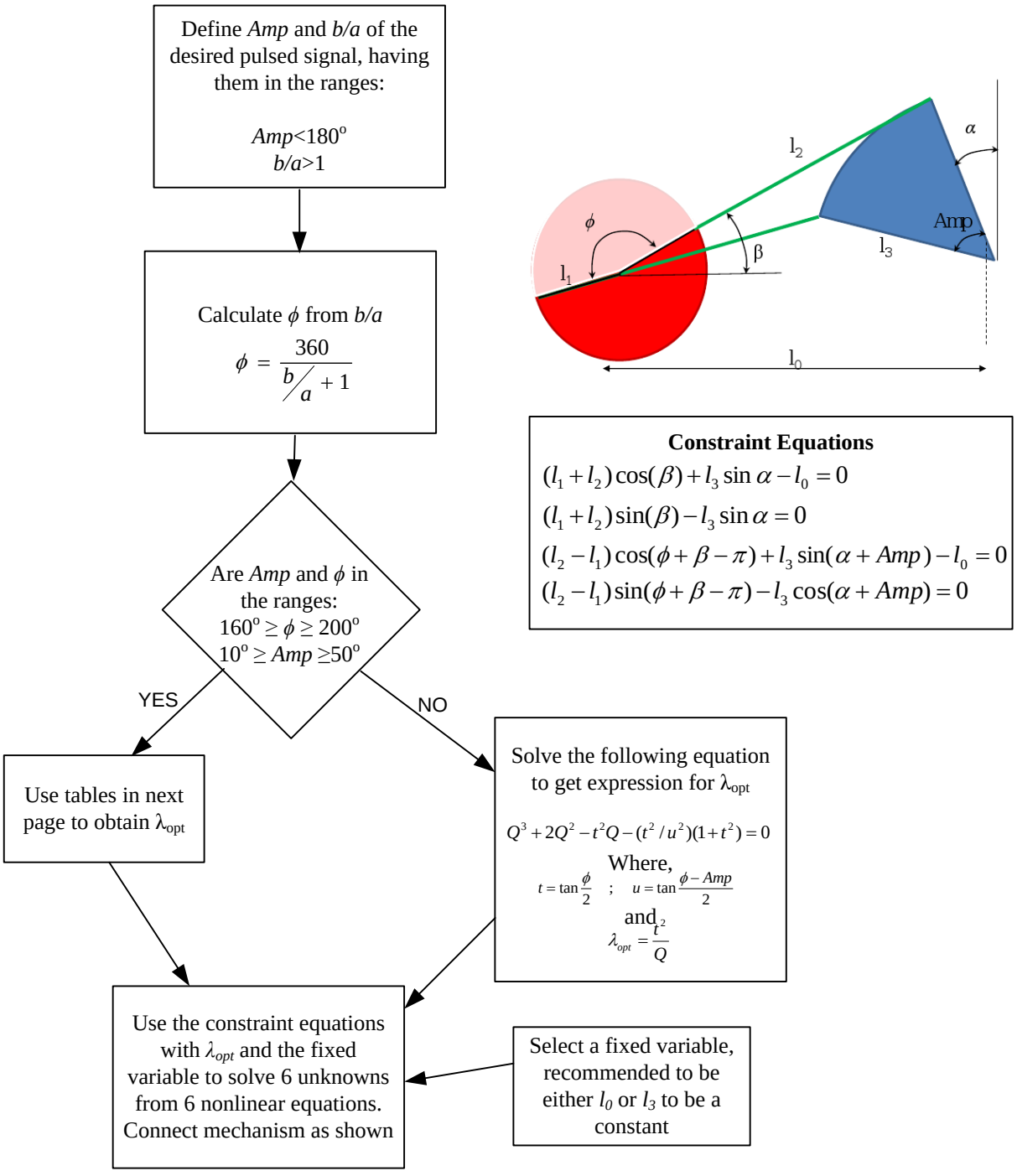

Figure B.1: Algorithm for choosing mechanism parameters

Optimum values of lambda ratio for given ø and ψ

ø deg	ψ, deg 160	162	164	166	168	170	172	174	176	178
10	2.3532	2.4743	2.6166	2.7873	2.9978	3.2669	3.6284	4.1517	5.0119	6.8642
12	2.3298	2.4491	2.5891	2.7570	2.9636	3.2272	3.5804	4.0899	4.9224	6.6957
14	2.3064	2.4239	2.5617	2.7266	2.9293	3.1874	3.5324	4.0283	4.8342	6.5387
16	2.2831	2.3988	2.5344	2.6964	2.8953	3.1479	3.4848	3.9675	4.7482	6.3853
18	2.2600	2.3740	2.5073	2.6664	2.8615	3.1089	3.4380	3.9080	4.6650	6.2427
20	2.2372	2.3494	2.4805	2.6368	2.8282	3.0704	3.3920	3.8499	4.5848	6.1087
22	2.2145	2.3250	2.4540	2.6076	2.7954	3.0327	3.3470	3.7935	4.5077	5.9826
24	2.1922	2.3010	2.4279	2.5789	2.7631	2.9956	3.3030	3.7388	4.4338	5.8641
26	2.1701	2.2773	2.4022	2.5505	2.7314	2.9594	3.2602	3.6857	4.3628	5.7524
28	2.1483	2.2539	2.3768	2.5227	2.7004	2.9239	3.2185	3.6344	4.2948	5.6469
30	2.1268	2.2309	2.3519	2.4954	2.6699	2.8893	3.1779	3.5847	4.2295	5.5472
32	2.1056	2.2082	2.3273	2.4685	2.6401	2.8554	3.1384	3.5367	4.1668	5.4526
34	2.0846	2.1858	2.3032	2.4421	2.6108	2.8223	3.0999	3.4901	4.1066	5.3628
36	2.0640	2.1637	2.2794	2.4162	2.5821	2.7899	3.0624	3.4449	4.0486	5.2773
38	2.0436	2.1420	2.2560	2.3908	2.5540	2.7583	3.0259	3.4012	3.9927	5.1957
40	2.0234	2.1205	2.2330	2.3657	2.5264	2.7274	2.9903	3.3587	3.9388	5.1177
42	2.0035	2.0994	2.2103	2.3411	2.4994	2.6971	2.9556	3.3175	3.8868	5.0430
44	1.9839	2.0785	2.1879	2.3169	2.4728	2.6675	2.9217	3.2773	3.8364	4.9712
46	1.9644	2.0579	2.1659	2.2931	2.4468	2.6384	2.8886	3.2383	3.7877	4.9023
48	1.9452	2.0375	2.1441	2.2696	2.4211	2.6100	2.8563	3.2003	3.7404	4.8358
50	1.9262	2.0174	2.1227	2.2465	2.3959	2.5820	2.8246	3.1632	3.6945	4.7717

Optimum values of lambda ratio for given ø and ψ

ø deg	ψ, deg 182	184	186	188	190	192	194	196	198	200
10	7.2086	5.3403	4.4560	3.9112	3.5318	3.2478	3.0245	2.8428	2.6911	2.5616
12	7.0369	5.2692	4.4227	3.8969	3.5282	3.2507	3.0317	2.8528	2.7030	2.5748
14	6.8646	5.1881	4.3795	3.8739	3.5174	3.2478	3.0341	2.8589	2.7117	2.5855
16	6.6971	5.1013	4.3287	3.8435	3.5000	3.2392	3.0317	2.8610	2.7171	2.5934
18	6.5371	5.0121	4.2726	3.8071	3.4768	3.2252	3.0245	2.8589	2.7189	2.5982
20	6.3857	4.9226	4.2131	3.7663	3.4487	3.2065	3.0129	2.8528	2.7171	2.5998
22	6.2431	4.8344	4.1518	3.7221	3.4167	3.1837	2.9972	2.8428	2.7117	2.5982
24	6.1090	4.7484	4.0900	3.6759	3.3818	3.1575	2.9780	2.8293	2.7030	2.5934
26	5.9830	4.6652	4.0284	3.6284	3.3447	3.1286	2.9558	2.8127	2.6911	2.5855
28	5.8644	4.5849	3.9676	3.5804	3.3062	3.0976	2.9311	2.7833	2.6763	2.5748
30	5.7527	4.5079	3.9080	3.5324	3.2669	3.0652	2.9045	2.7718	2.6592	2.5616
32	5.6472	4.4339	3.8500	3.4849	3.2272	3.0318	2.8764	2.7484	2.6399	2.5461
34	5.5475	4.3630	3.7936	3.4380	3.1875	2.9979	2.8473	2.7236	2.6190	2.5287
36	5.4529	4.2949	3.7388	3.3920	3.1480	2.9636	2.8175	2.6977	2.5967	2.5097
38	5.3631	4.2296	3.6858	3.3470	3.1089	2.9294	2.7873	2.6711	2.5734	2.4894
40	5.2776	4.1669	3.6345	3.3031	3.0705	2.8953	2.7570	2.6440	2.5492	2.4680
42	5.1960	4.1067	3.5848	3.2602	3.0327	2.8615	2.7266	2.6166	2.5246	2.4459
44	5.1180	4.0487	3.5367	3.2185	2.9956	2.8282	2.6964	2.5891	2.4996	2.4232
46	5.0432	3.9928	3.4901	3.1779	2.9594	2.7954	2.6665	2.5617	2.4744	2.4001
48	4.9715	3.9389	3.4450	3.1384	2.9239	2.7631	2.6369	2.5344	2.4491	2.3767
50	4.9025	3.8869	3.4012	3.0999	2.8893	2.7314	2.6076	2.5073	2.4239	2.3533

Figure B.2: Tables to choose λ_{opt} for algorithm

B.3 Control Motor Specifications

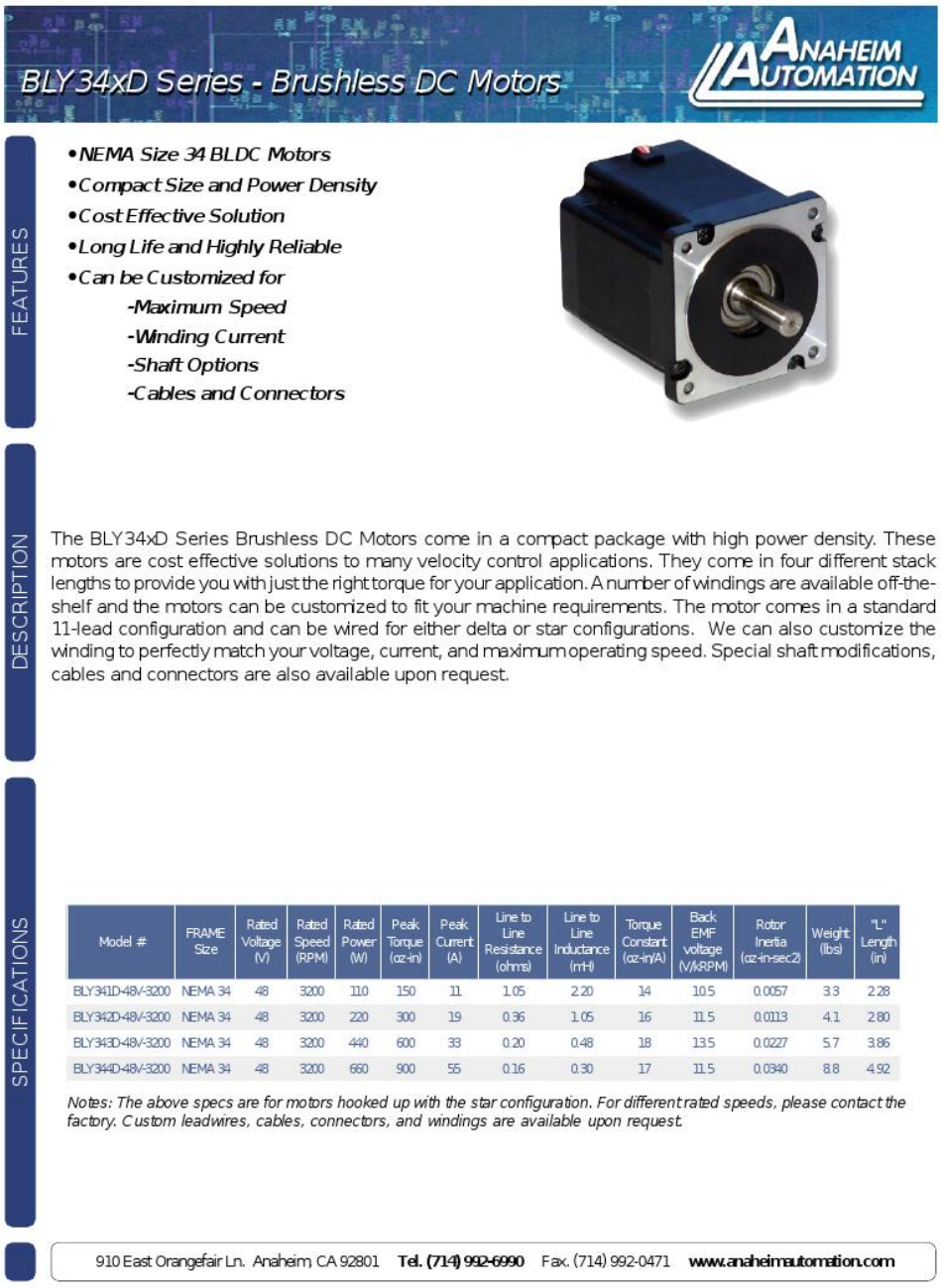

BLY34xD Series - Brushless DC Motors

ANAHEIM AUTOMATION

FEATURES

- NEMA Size 34 BLDC Motors
- Compact Size and Power Density
- Cost Effective Solution
- Long Life and Highly Reliable
- Can be Customized for
  - -Maximum Speed
  - -Winding Current
  - -Shaft Options
  - -Cables and Connectors

DESCRIPTION

The BLY34xD Series Brushless DC Motors come in a compact package with high power density. These motors are cost effective solutions to many velocity control applications. They come in four different stack lengths to provide you with just the right torque for your application. A number of windings are available off-the-shelf and the motors can be customized to fit your machine requirements. The motor comes in a standard 11-lead configuration and can be wired for either delta or star configurations. We can also customize the winding to perfectly match your voltage, current, and maximum operating speed. Special shaft modifications, cables and connectors are also available upon request.

SPECIFICATIONS

Model #	FRAME Size	Rated Voltage (V)	Rated Speed (RPM)	Rated Power (W)	Peak Torque (oz-in)	Peak Current (A)	Line to Line Resistance (ohms)	Line to Line Inductance (mH)	Torque Constant (oz-in/A)	Back EMF voltage (V/kRPM)	Rotor Inertia (oz-in-sec2)	Weight (lbs)	"L" Length (in)
BLY341D-48V-3200	NEMA 34	48	3200	110	150	11	1.05	2.20	14	10.5	0.0057	3.3	2.28
BLY342D-48V-3200	NEMA 34	48	3200	220	300	19	0.36	1.05	16	11.5	0.0113	4.1	2.80
BLY343D-48V-3200	NEMA 34	48	3200	440	600	33	0.20	0.48	18	13.5	0.0227	5.7	3.86
BLY344D-48V-3200	NEMA 34	48	3200	660	900	55	0.16	0.30	17	11.5	0.0340	8.8	4.92

Notes: The above specs are for motors hooked up with the star configuration. For different rated speeds, please contact the factory. Custom leadwires, cables, connectors, and windings are available upon request.

910 East Orangefair Ln. Anaheim, CA 92801 **Tel. (714) 992-6990** Fax. (714) 992-0471 **www.anaheimautomation.com**

Figure B.3: Control motor detail and specifications